buildings

MDPI

Article

Cooling Heritage Scenarios: Transforming Historic Squares for Thermal Comfort

Pegah Rezaie [1], Victoria Patricia Lopez-Cabeza [2], Javier Sola-Caraballo [1,3] and Carmen Galan-Marin [1,3,*]

[1] Departamento de Construcciones Arquitectónicas I, Escuela Técnica Superior de Arquitectura, Universidad de Sevilla, 41012 Seville, Spain; pegrez@alum.us.es (P.R.); jdesola@us.es (J.S.-C.)
[2] Centro de Investigación en Tecnología, Energía y Sostenibilidad, Universidad de Huelva, 21810 Huelva, Spain; vlopez7@us.es
[3] Instituto Universitario de Arquitectura y Ciencias de la Construcción, Universidad de Sevilla, 41012 Seville, Spain
* Correspondence: cgalan@us.es

Abstract: Urban squares in historic neighborhoods are vital public spaces, often the only nearby option available for an aging population. However, these spaces face increasing thermal discomfort exacerbated by urban heat island (UHI) effects. This research focuses on improving thermal comfort for two case studies located in Seville's high-density and historically rich Casco Antiguo neighborhood. Although their significance and social value make them central meeting points for locals and visitors, these squares face major challenges regarding thermal comfort, mainly due to a lack of greenery or adequate shading. This study examines the conditions by conducting in-person monitoring and simulations, identifying factors contributing to discomfort. On the basis of this, the research proposes mitigation strategies to address these issues. These solutions include the installation of green walls, the addition of canopies, and the application of specific surface materials to improve the conditions of these squares. Canopies provided the most significant cooling, reducing universal thermal climate index (UTCI) values by up to 6.5 °C. Green walls delivered localized cooling, lowering the mean radiant temperature (MRT) by up to 5 °C. The results reveal how these approaches can bring about changes in thermal comfort in a way that benefits historic city environments.

Keywords: thermal comfort; heritage conservation; historic neighborhoods; mitigation strategies; urban heat island (UHI); urban intervention; ENVI-met simulation

check for updates

Academic Editor: Elena Lucchi

Received: 8 January 2025
Revised: 7 February 2025
Accepted: 8 February 2025
Published: 12 February 2025

Citation: Rezaie, P.; Lopez-Cabeza, V.P.; Sola-Caraballo, J.; Galan-Marin, C. Cooling Heritage Scenarios: Transforming Historic Squares for Thermal Comfort. *Buildings* **2025**, *15*, 564. https://doi.org/10.3390/buildings15040564

Copyright: © 2025 by the authors. Licensee MDPI, Basel, Switzerland. This article is an open access article distributed under the terms and conditions of the Creative Commons Attribution (CC BY) license (https://creativecommons.org/licenses/by/4.0/).

1. Introduction

The expansion of urban areas, fueled by the rising migration of individuals to cities, currently home to half the global population, is forecast to continue in the coming years. At the beginning of the 21st century, urbanization has sped up notably as over half of the population currently lives in cities; this figure is expected to increase to around 60% by 2030 [1]. The clustering of populations in urban areas amplifies the urban heat island (UHI) effect [2], which becomes more pronounced with increasing population density and environmental changes [3–5].

The development and operation of urban areas play a crucial role in shaping the overall well-being of citizens [6]. According to research, average temperatures in urban centers worldwide could rise by 1.4–4.8 °C by the end of the 21st century [7]. Consequently, cities are becoming increasingly vulnerable to the effects of urbanization and climate change, which include elevated temperatures and concentrated pollution. As the population

grows and the proportion of open areas in the cities decreases, especially in city centers, there is a growing demand for high-quality outdoor areas offering healthy recreational amenities [8]. These spaces play a crucial role in enhancing the livability and vibrancy of urban environments. Encouraging increased use of outdoor spaces can yield substantial benefits to the physical, environmental, economic, and social aspects of cities [9].

Outdoor thermal comfort measures the perception that expresses satisfaction with the surrounding outdoor thermal environment. This is influenced by a number of factors, including air temperature (AT), relative humidity (RH), wind speed (WS), solar radiation, and the presence of shading or greenery [10]. In addition to the climatic variables, urban design elements such as building shape [11], materials [12], and vegetation [13] influence outdoor thermal comfort [14]. However, the feeling of comfort differs among individuals, as it is influenced by personal variables such as how people are feeling on a given day or their cultural and social background [15]. Nevertheless, in this case, climate takes the lead in shaping the level of health and satisfaction humans feel in relation to their surrounding environment [16,17]. Human biometeorology research is heavily dependent on an understanding of how climate impacts human thermal comfort, well-being, and mental performance [18].

The universal thermal climate index (UTCI) team's multidisciplinary approach [19] was a significant departure from past efforts to understand thermal indices—often isolated endeavors. Collaborative research was fostered by integrating insights from various fields, leading to a universal solution for assessing human thermal environments. This project, housed within an International Society of Biometeorology Commission and a European COST Action, established an international framework for standardizing the UTCI as a climatic index [19]. UTCI applies advanced modeling techniques to evaluate outdoor thermal conditions, simulating physiological responses of the human body, taking into consideration factors such as clothing and environmental elements such as humidity, radiation, and wind [20]. The operational procedure, available as software on the UTCI website [21], demonstrates credible assessments of thermal conditions in hot and cold environments, aligning closely with existing standards [22–24].

Urban areas experience notable fluctuations in thermal comfort due to changes in the radiation balance, wind flow, the layout of buildings [25], and urban features [26] such as vegetation [27]. These variations create microclimate scenarios over periods that impact how people perceive local thermal comfort [28]. Green and open spaces play a role in enhancing environments and creating attractive city landscapes [29–31]. Since the 1980s, growing concerns about residents' well-being have prompted an increase in research into the comfort of people in urban spaces such as parks and squares [32]. This trend has led to studies focusing on creating microclimates to improve the comfort of pedestrians [33]. As visitors are more likely to use urban spaces when they are comfortable, outdoor thermal comfort plays a crucial role in how these locations are utilized [34].

Several methods have been used in previous studies to mitigate the impact of heat in urban areas, improving thermal comfort [35–37]. These methods could be classified by strategy [38], with the most common and successful being: 1. the modification of surface properties to increase reflection and reduce heat storage [39,40]; 2. the provision of shade to decrease solar radiation absorption [39]; 3. the use of green structures to increase RH while reducing AT; 4. the enhancement of urban airflow [41]; and 5. the utilization of active cooling techniques such as water and ground cooling [39,42]. Numerous examples can be found in the literature on the effectiveness of these strategies, either individually or in combination.

The concept of albedo, representing the proportion of solar radiation reflected by a surface compared to the total amount received, significantly influences the thermal

properties of ground surfaces and the UHI effect [43]. The effectiveness of supercool materials depends on factors such as heat capacity, the potential amount of heat stored; solar reflectance, the amount of sunlight reflected; heat transfer rates, the speed at which heat moves through these; surface roughness; and permeability, showing how easily water can pass through these materials. Although high-albedo material is an extremely promising strategy, some studies suggest it can harm thermal comfort as a result of an increased mean radiant temperature (MRT) [44]. In order to achieve the highest thermal comfort possible, albedo must be optimized for each case.

Furthermore, the effect of adding vegetation is two-fold: it offers shade-blocking direct solar radiation, while green evapotranspiration reduces AT. Green structures play a crucial role in mitigating thermal conditions. Studies indicate that surfaces covered with greenery experience cooler temperatures than surfaces made of artificial materials such as concrete and asphalt [39], even if the albedo values are similar. Conversely, trees can serve as barriers against wind currents, potentially hindering heat dissipation [45]. Complementary to vegetation, artificial canopies such as sun sails or other textile membranes help reduce solar radiation without increasing RH or excessively hindering wind flow [4,46].

While urban geometry can influence how heat moves through areas because of radiation and convection procedures, design results are crucial to determining the wind flow velocity and direction [47]. Water bodies and irrigations can usefully help to cool spaces through evaporation and their high heat capacity. Although the cooling effects of bodies of water depend on aspects such as size, shape, position, wind patterns, and nearby buildings and structures, in general, the literature notes a considerable potential AT reduction [38]. However, these lead to a waste of a high volume of water, which could be detrimental in dry regions.

The evaluation of the mitigating capacity of some of the strategies above has been addressed previously [38]. Some of these experimental studies measure the effects of the application of specific techniques. Various studies have focused on [48] materials and their properties, demonstrating the great potential of the use of cooling materials [49] and resulting in reductions in surface temperature (ST) of up to 10 °C. Furthermore, other experiments [50] have been conducted by combining strategies in defined spaces, also providing promising results with reductions of up to 11 °C in transitional spaces. Despite the particular difficulties presented by the evaluation of materials in larger urban spaces, successful examples can be found in other studies [51], where a considerable reduction in temperature (4 °C) is observed in experimental urban spaces.

The difficulties mentioned above have contributed to the increased relevance of computational simulations. Computational Fluid Dynamics (CFD) programs such as ENVI-met [51] facilitate simulated experimentation based on scientific data, in turn reducing costs. Numerous studies have evaluated various mitigation strategies (MS) using ENVI-met simulations [38]. In some cases, theoretical possible scenarios explicitly designed for experimentation have been evaluated [52,53]. However, other evaluations examined real case studies [54], increasing the direct contextual applicability of results. This has resulted in a UTCI reduction of 6 °C in urban parks thanks to the use of greenery. In other studies focused on historical-heritage areas [55,56], mitigation scenarios have been tested and evaluated in complex areas, albeit on a large scale, without a particularly detailed examination of representative small spaces within the historic center studied.

In contrast, recent studies have focused on the use of innovative materials with great cooling potential, including facade materials, making them doubly beneficial. Santamouris and Yun [57] emphasize the potential of innovative materials, such as photonic, thermochromic, and PCM-doped surfaces, in mitigating UHI effects. Their research confirms

that these materials can substantially reduce the ST, occasionally achieving sub-ambient levels and lower temperatures than conventional materials.

However, the protection of the urban fabric and configuration in historic cities is a crucial aspect of urban planning and heritage conservation, as seen in previous research [58]. It involves preserving the unique spatial structures, architectural styles, and cultural significance of historic areas while taking into account modern development needs, as highlighted in studies on traditional urbanism and housing [59,60]. These works illustrate how traditional architectural solutions align with local environmental conditions while preserving cultural identity. This principle is essential when developing climate-responsive strategies for historic urban squares. The evaluation of thermal comfort in these scarce communal spaces goes beyond mere luxury and can be considered indispensable when fostering an environment conducive to social gatherings and community interactions, given the importance of these squares to the well-being of citizens.

Seville, a city in the south of Spain, is famous for its historic center. The *Casco Antiguo*, or Old Town, of Seville is one of the largest in Europe, covering approximately 4 square kilometers. Known for its well-preserved architecture and vibrant cultural heritage, Old Town is a large, sprawling historic area. The city of Seville, known for having some of the highest temperatures not only in Spain but also in Europe [61], has been selected to develop a methodology for assessing thermal comfort in historic squares based on detailed analysis. A previous study [61] has found that Seville's Old Town is cooler than the periphery during the day. However, due to its high density, it is more prone to suffer from the UHI effect at night. This is why, due to its high density, urban heat mitigation interventions are difficult to undertake. Expansion and relaxation spaces, such as squares, offer the most opportunities for public space improvement.

This analysis provides a thorough assessment of various factors influencing comfort levels. Numerical simulations, conducted using ENVI-met software, play a significant role in this appraisal, focusing on understanding the effect on thermal comfort of factors such as the AT, RH, WS, and MRT in the squares. This article further explores the multifaceted aspects of thermal comfort assessment in increasing heat conditions affecting historic city squares. It follows a comprehensive approach that integrates empirical analyses, simulation techniques, and innovative solutions. These are applied in a historic heritage city center, where the characteristic urban fabric, the dilatations in the form of small squares, and the traditional construction system play a crucial role in the thermal performance and perception of social space. The interventions must, therefore, take these problematic considerations into account.

Thus, the research is structured as follows: an initial methodology is presented, which includes the case study description, the field measurements, and the setup for the ENVI-met simulation of the various scenarios. The results are then organized by scenarios within each specific case study before being discussed from various perspectives and presenting the final conclusions.

2. Materials and Methods

This study proposes MSs for the typical urban squares located in a historic city such as Seville in order to improve users' thermal comfort under extremely hot conditions. The two case studies selected in Seville have been monitored to calibrate the simulation software, modeling different strategies in order to propose the optimal strategy. The following methodological flow has been summarized in Figure 1.

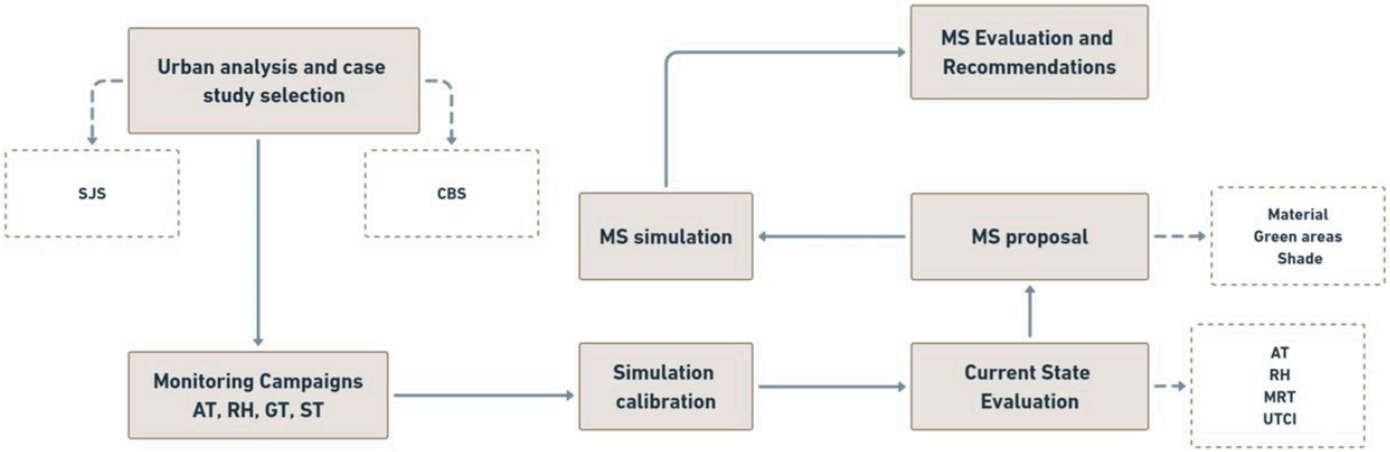

Figure 1. Methodology flowchart.

2.1. Research Philosophy and Strategy

This study adopts a pragmatic research philosophy, focusing on real-world applications and the integration of quantitative data (e.g., recorded climatic data and ENVI-met simulations) in order to propose specific MSs for thermal comfort with quantitative results. The case study approach selected aimed to emphasize two representative historic squares in Seville. It includes a detailed examination of the microclimatic conditions and the impact of proposed interventions within the study area's unique historical and cultural contexts. The research employs a mixed-method approach, combining observational data, numerical simulation, and a comparative analysis of baseline and mitigated scenarios. Based on this combination, a comprehensive understanding of thermal behavior and the effectiveness of the strategies proposed can be guaranteed.

2.2. Time Horizon, Data Collection Techniques, and Analysis Tools

This study, which focuses on warm climates, examines the initial data, simulations, and results for a representative summer day (23 July 2023) in order to capture peak thermal conditions, providing a snapshot of the extreme heat impact in the case study areas. Climate data were collected from official meteorological records, while on-site measurements with calibrated instruments were used to calibrate the simulation process. Statistical validation metrics, including calculated statistical errors, were employed to evaluate the accuracy and reliability of the simulation results. The data analysis incorporates ENVI-met software to simulate microclimatic conditions under baseline and to propose mitigation scenarios.

2.3. Case Studies

Located in Spain at 37.3891° N, 5.9845° W, with an average elevation of 6 m above sea level, Seville covers 141.28 km^2. It is characterized by a Mediterranean climate with hot, dry summers and mild winters. The average annual temperature is approximately 19 °C, although summer highs frequently exceed 35 °C (104 days in 2023), and on multiple occasions each year, temperatures remain above 40 °C for several consecutive days [62].

According to a previous study and classification [61], Seville has numerous high-density residential neighborhoods. The most prominent of these, Casco Antiguo, serves as the historic center of Seville. Casco Antiguo is still densely populated and characterized by narrow streets and traditional architecture, consisting of a mix of residential buildings, shops, and tourist attractions. Even though large green spaces are conspicuously absent, several small hard-paved squares found in the area serve as gathering spots for residents and visitors. The study of these spaces is particularly important for improving thermal

comfort in hot weather, given the potential risks posed by elevated temperatures to public health and the usability of these areas.

Two squares, considered typical urban archetypes of historic cities in Mediterranean climates, in this case Seville, have been selected. Both squares share standard features, such as compact urban morphology, high-density surroundings with traditional constructive systems [58], and limited green infrastructure, all traits frequently found in historic city centers across southern Europe (Figure 2):

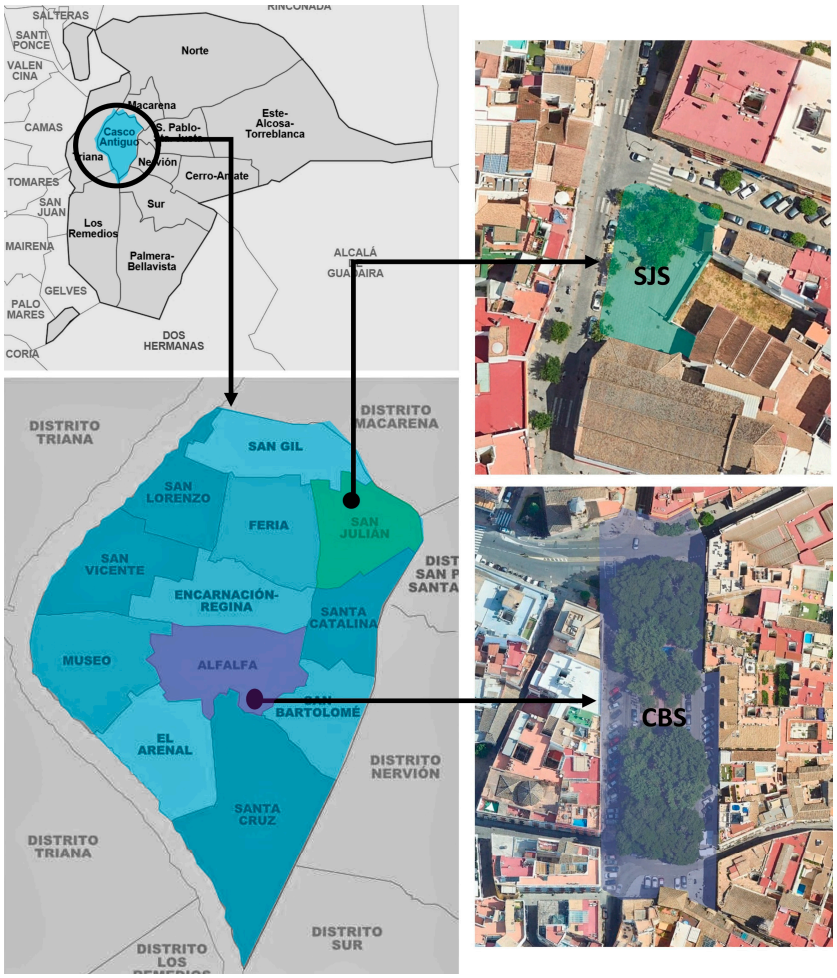

Figure 2. Casco Antiguo neighborhood and San Julian Square (SJS) and Cristo de Burgos Square (CBS) locations.

- San Julian Square (SJS) has been chosen for the assessment of thermal comfort, as its shape, design features, and lack of water elements and greenery are also a feature of many small squares nearby. SJS is approximately 28.5 m wide and 44 m long, while the surrounding buildings average a height of 9.5 m. Traditional construction techniques have played a crucial role in shaping the thermal properties of these squares: the surrounding facades are primarily made of local traditional mass bricks, with mortar render painted in light colors, while the roofs are ceramic tiles. Granite cobblestone covers the road surrounding two sides of the square, while the pathways are paved in cement mortar tile or stone tiles, as shown in Figure 3. The cobblestones, laid using compacted sand beds and interlocked with mortar, provide stability but lack permeability and contribute to surface heating.

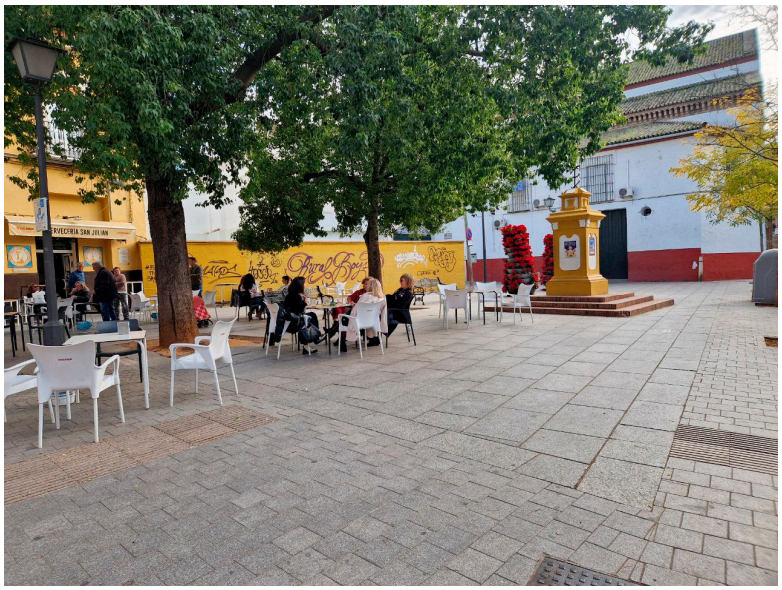

Figure 3. General view of SJS.

- In contrast, Cristo de Burgos Square (CBS) has an abundance of vegetation. The square, which is 40.2 m wide and 132.9 m long, is surrounded by buildings with a height of 10.5 m. The materials of surrounding buildings are also traditional mass brick walls with mortar render and light paint colors, while the roofs still use ceramic tiles. On the ground, an asphalt road surrounds the square, while the pedestrian area is paved with red brick tile (Figure 4). The dimensions and materials significantly influence the area's environmental situation. The design elements of the square—mostly existing greenery that provides shade—play an essential part in shaping visitors' thermal experiences and will guide us in analyzing its microclimate and comparing it with the previous one of both squares. Valuable input on thermal standards can be obtained thanks to the potential perception of variables such as solar exposure and wind flow positioning. CBS features red brick tiles laid over concrete layers, which enhance durability but restrict natural cooling mechanisms. However, in their current form, these historically authentic methods limit thermal mitigation options.

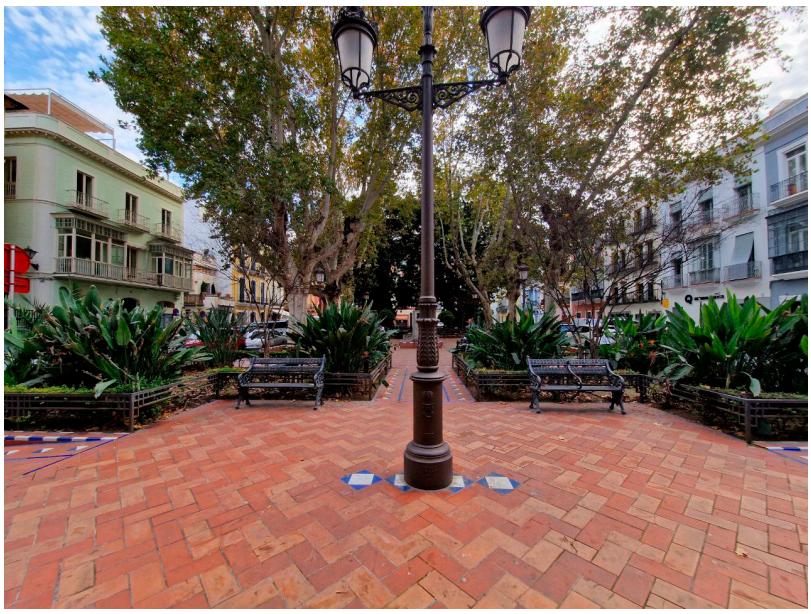

Figure 4. Central perspective of CBS.

2.4. Field Measurements

Field measurements are crucial for validating the accuracy of simulations within the research site. Data collection was conducted at different times in the two squares on a representative summer day (23 July 2023). The AT, RH, and globe temperature (using a TROTEC TC100 thermo-hygrometer), WS (using a TROTEC TA300 anemometer), and ST (using a TESTO 905 T2 thermometer) were measured. Ten points were selected in each of these squares for the purposes of measurement (Figure 5). These data are used to calibrate the ENVI-met simulation models, enabling the simulation of microclimate and thermal comfort under different configurations of the MS. A summary of the technical specifications of the instruments used can be found in Table 1.

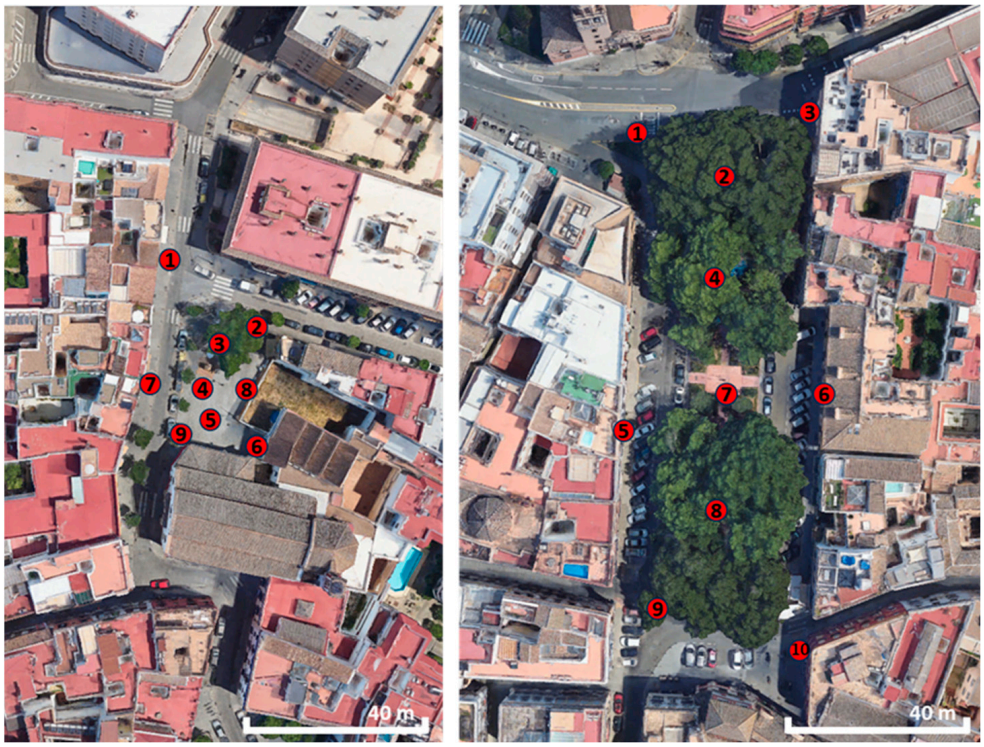

(**a**) SJS (**b**) CBS

Figure 5. Selected measurement points in SJS and CBS.

Table 1. Measuring instruments specifications.

Instrument and Model	TROTEC TC100 Thermo-Hygrometer	TROTEC TA300 Anemometer	Testo 905 T2 Thermometer
Range	Temperature: −20 °C to 60 °C Humidity: 1% to 99% RH	Wind Speed: 0.4 m/s to 30 m/s Air Velocity: 0.4 m/s to 30 m/s Temperature: −20 °C to 60 °C	−50 °C to 300 °C
Accuracy	Temperature: ±0.5 °C at 25 °C Humidity: ±3% RH (at 25 °C, 30% to 80% RH); ±5% RH (at 25 °C, <30% RH or >80% RH)	Wind Speed/Air Velocity: ±3% of reading ±0.1 m/s Temperature: ±0.8 °C	±1 °C (−50 °C to −20.1 °C); ±0.5 °C (−20 °C to 99.9 °C); ±1% of reading (remaining range)
Resolution	Temperature: 0.1 °C Humidity: 0.1% RH	Wind Speed/Air Velocity: 0.1 m/s Temperature: 0.1 °C	0.1 °C
Operating Environment	Temperature: 0 °C to 50 °C Humidity: 0% to 95% RH (non-condensing)	Temperature: 0 °C to 50 °C Humidity: 0% to 80% RH (non-condensing)	temperature: −20 °C to 50 °C

2.5. Simulation Setup

ENVI-met is designed to examine microclimates by applying the foundational principles of fluid dynamics and thermodynamics [63]. It can replicate the intricate interplays

among buildings, soil, greenery, and the atmosphere. It, therefore, has widespread use in research on urban microclimates. The software is tailored for 3D modeling, featuring a typical horizontal resolution in a 0.5–5 m range and a temporal scope of 24 to 48 h, using time steps of 1 to 5 s. This level of resolution facilitates the scrutiny of interactions among individual buildings, surfaces, and vegetation [64]. The ENVI-met simulations were designed to assess the thermal behavior of the selected squares, further enriched by incorporating observations from field studies. Once the on-site measurements had been obtained, simulations were conducted on the thermodynamic performance of the squares using the ENVI-met software (version 5.1.1). Details relating to the models and boundary conditions for the simulated squares are outlined and presented in Tables 2 and 3.

Table 2. Simulation model dimensions and geometry specifications.

Parameters	SJS	CBS
Number of grid cells	80 × 70 × 15	100 × 105 × 30
Size of the cells (m) (x,y,z)	2 × 2 × 2	2 × 2 × 2
Nesting grids	4	4
Model rotation out of north	0	0
Telescoping factor (%)	15	15
Telescoping starts after height (m)	20	20
Image of the model	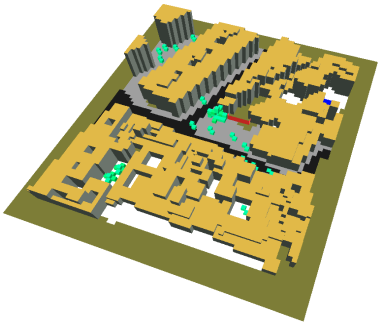	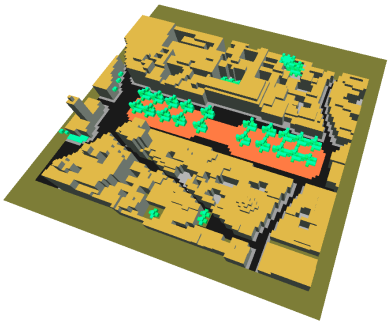

Table 3. Input variables for ENVI-met simulations.

Meteorological inputs	Air temperature and relative humidity Wind speed and direction Specific humidity at 2500 m Roughness length	Hourly data in Table 4 1 m/s = 191.73° 8.0 g/kg 0.01 m
Vegetation	3D tree Simple plant	02SSSS, 02ALDM, 02ALDS (SJS) 0200XX, 020027, 010027, 01PLDM, 02ALDM, 02ALDS (CBS)
Building	Walls and roof materials	Table 5
Soil	Initial conditions for soil materials (Table 5)	Upper layer (0–20 cm): 65%/20 °C Middle layer (20–50 cm): 70%/20 °C Deep layer (50–200 cm): 75%/19 °C
Simulation	Start simulation day (DD.MM.YYYY) Start simulation time (HH:MM: SS) Total simulation time (hours)	22.07.2023 21.00.00 28 h

The simulations were conducted on the same day of the monitoring campaigns, 23 July 2023. The simulation input parameters included an hourly AT and RH using simple forcing, along with the average WS and direction taken from a nearby weather station within the city, 3.5 km from the squares (Table 4).

Table 4. Hourly air temperature and relative humidity recorded by the official weather station on 23 July 2023.

Hour	AT (°C)	RH (%)	Hour	AT (°C)	RH (%)	Hour	AT (°C)	RH (%)	Hour	AT (°C)	RH (%)
0:00	25.3	43	6:00	21.7	67	12:00	29.2	41	18:00	36.5	18
1:00	23.6	49	7:00	21.6	66	13:00	31.1	37	19:00	37.4	18
2:00	22.7	58	8:00	22.1	66	14:00	32.9	31	20:00	36.5	19
3:00	22.5	64	9:00	24.1	61	15:00	34.8	26	21:00	34.5	24
4:00	21.7	65	10:00	26.3	54	16:00	36.0	24	22:00	32.0	32
5:00	21.8	67	11:00	27.5	49	17:00	36.3	26	23:00	29.7	37

The MSs proposed in this study are mainly based on material modifications, vegetation, and shade. Table 5 describes the properties of the materials used in the simulation models. Materials for the MSs are classed as either currently in place or proposed and are described in the following sections.

Table 5. Material properties specified in the simulation model.

Property/Material	Absorp.	Transmis.	Albedo	Emissiv.	Vol. Heat ($(J/(m^3 \cdot K)) \times 10^6$)	T.Conduct. (W/(m·K))	Density (kg/m^3)	Z0 Roughness Length (m)
Existing materials								
Asphalt	0.88	-	0.12	0.90	2.251	0.90	-	0.010
Concrete	0.50	-	0.50	0.93	2.083	1.63	-	0.010
Red cobblestone	0.70	-	0.30	0.90	2	1.00	-	0.010
Granite pavement	0.65	-	0.35	0.90	2.345	3.10	-	0.010
Natural soil	0.80	-	0.20	0.90	1.320	0.00	-	0.015
Proposed materials								
Clear permeable concrete	0.50	-	0.50	0.93	1.750	1.00	-	0.010
Paved grass	0.70	-	0.30	0.97	0.836	0.00	-	0.015
Textile shade	0.20	0.30	0.50	0.70	Specific Heat 1500 J/(kg K)	0.19	350	0.020

2.6. Performance Parameters

As this study aims to evaluate and propose MSs to improve thermal comfort in historic squares, different climatic and comfort parameters are selected in order to assess the performance of the case studies. These parameters are the AT, RH, WS, MRT, and UTCI. These variables are measured 1.4 m above the ground (the height of an individual) and represented on thermal maps at different times (6:00, 12:00, 16:00, and 20:00), with hourly graphs selecting specific points in the squares. Five representative points were chosen for an in-depth analysis of the microclimate variables of both squares. Figure 6 shows the location of the points selected. Point 1, lacking any shade, is situated northwest of SJS. Point 2 is located under the shade of vegetation. Point 3 is exposed to sunlight near the empty wall and has poor visibility. Point 4 is the central position within the square, where gatherings typically occur. Finally, point 5, in the southeast corner of the square, is positioned under the shade of surrounding buildings (Figure 6a).

In CBS, point 1 was chosen due to its location in the northern part of the square, shaded by vegetation. Point 2 was selected for its position within the playground with different ground materials. Point 3 was chosen for its position at the center of the square, where gatherings occur, and lacks vegetation shading. Point 4 was selected for being under the densely populated canopy of the bar. Point 5 was chosen for its position in the square's southwest corner on asphalt ground (Figure 6b).

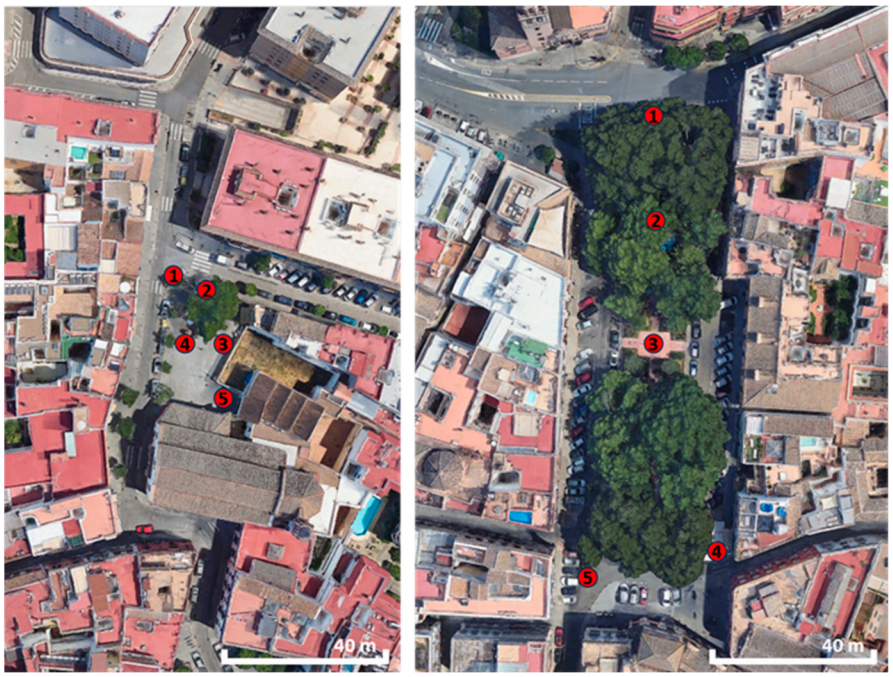

(**a**) SJS (**b**) CBS

Figure 6. Selected analysis points in SJS and CBS.

2.7. Calibration of the Models

When evaluating how well a simulation can reproduce reality, this study considers four measures: Normalized Mean Bias Error (NMBE), Mean Absolute Percentage Error (MAPE), Root Mean Square Error (RMSE), and Coefficient of Variation of the Root Mean Square Error (CV(RMSE)). These measures are commonly used to assess the reliability of forecasting or prediction models [65]. The ideal value for these parameters, used to signify similar simulations and measurements, is 0. Usually, CV(RMSE) values under 30% and NMBE values under 10% are considered acceptable. The parameters compared to calculate these statistical errors were the AT, RH, MRT, and UTCI.

2.8. Mitigation Strategies

The current state (CS) and MS for both squares are presented. Four simulation cases are provided, with two scenarios per square: SJS-CS (the current state of San Julian Square), SJS-MS (the mitigation strategies scenario for San Julian Square), CBS-CS (the current state of Cristo de Burgos), and CBS-MS (the mitigation strategies scenario for Cristo de Burgos Square).

The Results section details the SJS-CS, providing an assessment of discomfort at various points, which are then discussed in the following section. Decisions were made regarding specific strategies for addressing discomfort, to be evaluated using ENVI-met simulations. Taking into consideration the characteristics of this square and the space limitations for new vegetation, a green wall is proposed to enhance the visual aesthetics and utilize vegetation to promote cooling by evapotranspiration. The significant constraints on space encountered in SJS make it impractical to add new trees or large vegetation. Vertical vegetation is thus considered appropriate for this square.

The addition of paved grass along both sides of the square is proposed to reduce the ST, which tends to be higher due to the heat absorption by conventional paving materials. This element can be walked on and is suitable for areas with limited space, making it ideal for maintaining accessibility. Combining both thermal performance and practicality, it addresses the cooling needs as well as pedestrian functionality.

Additionally, the installation of temporary canopies is proposed. Given the small size and lack of natural shading in the square, temporary canopies are proposed to reduce solar radiation exposure immediately. Temporary canopies provide a flexible, non-invasive solution that preserves the historical and cultural significance of the square. Furthermore, their visual impact is minimized during the cooler months since they can be installed seasonally (Figure 7).

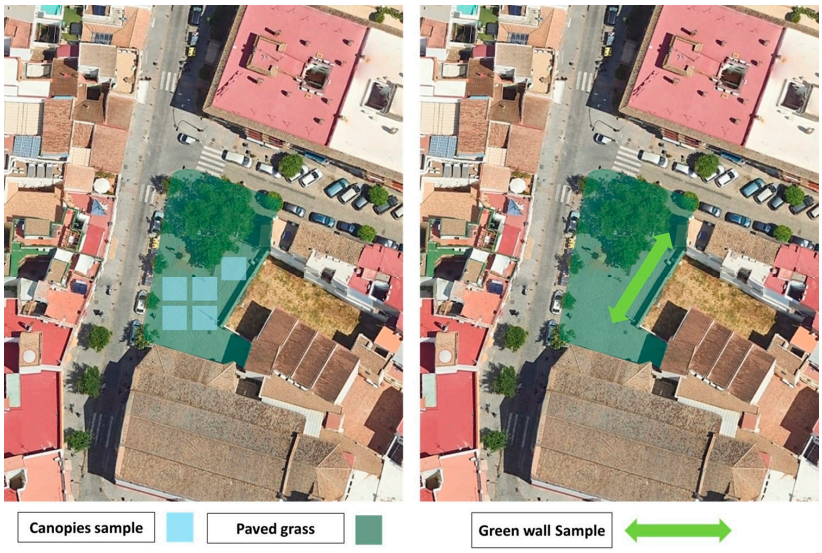

Figure 7. Mitigation strategies proposal for San Julian Square.

In the case of CBS, the existing vegetation already makes the square very shaded and relatively cool. For this reason, the MS focuses on materials and shading. The substitution of hard pavement for paved grass is proposed in many parts of the square, especially around the existing trees. Temporary canopies are also proposed for areas not covered by trees (Figure 8).

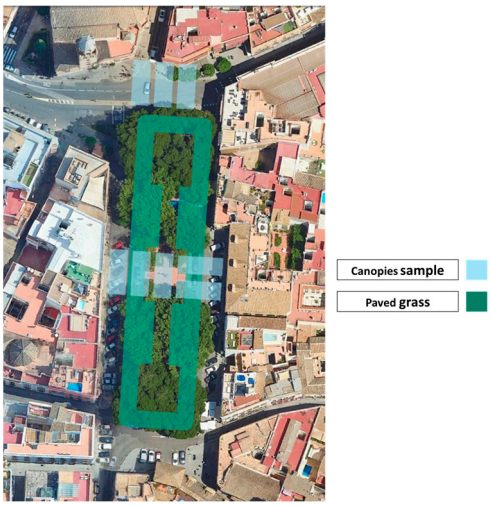

Figure 8. Mitigation strategies proposal for Cristo de Burgos Square.

3. Results

This section presents the results of the monitoring and simulations. The monitoring results shown initially are followed by a discussion on the validation of the simulations. Finally, the simulation results for the CSs and MSs for both squares are presented.

3.1. Monitoring Results

The monitoring reveals variations in AT, RH, WS, and ST between the two squares.

Due to equipment and accessibility restrictions, the monitoring times differed between both squares. In SJS, measured at 18:00 h, the lowest AT was 37.9 °C while the highest temperature was 40.8 °C (Figure 9a). In CBS, which was measured at 13:00 h, the minimum AT was 33.0 °C and the maximum temperature was 37.4 °C (Figure 9b). The highest variations were identified between points in the sun and those in the shade.

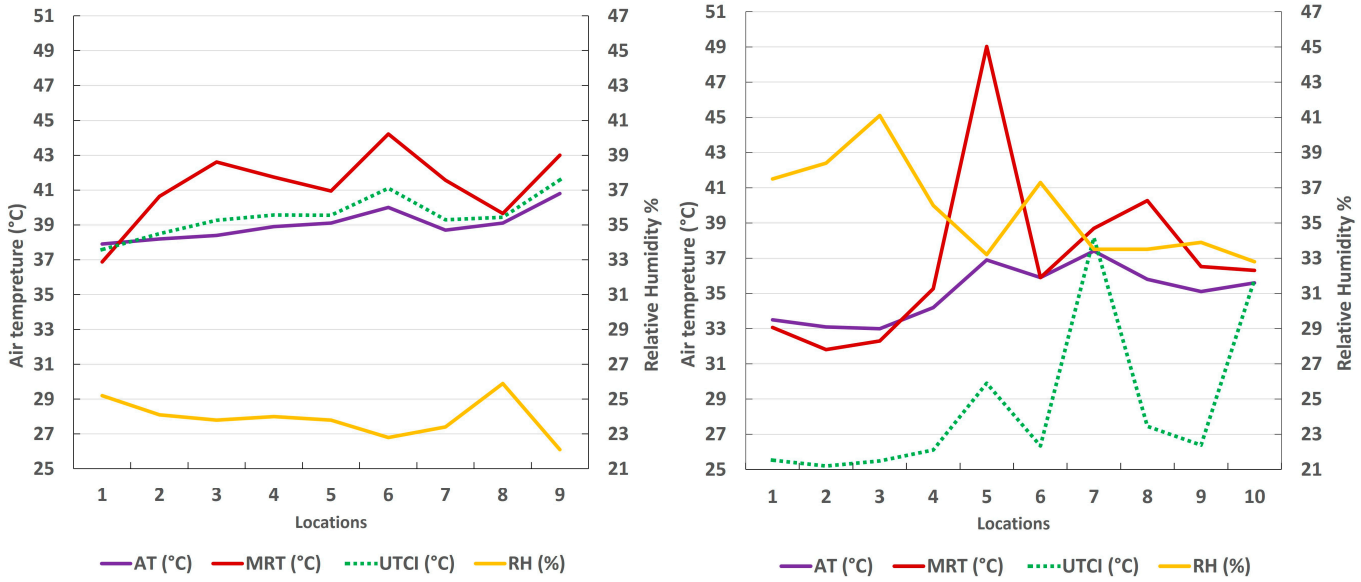

(**a**) SJS at 18:00 h (**b**) CBS at 13:00 h

Figure 9. The monitoring results of the case studies: (**a**) the SJS air temperature and relative humidity were measured, and the MRT and UTCI were calculated in 9 locations. (**b**) The CBS air temperature and relative humidity were measured, and the MRT and UTCI were calculated in 10 locations.

Both squares displayed low WS values, between 0.7 and 1.5 m/s. These values are attributed to the high urban density in these areas and the vegetation blocking the WS.

STs were measured in order to analyze the difference between materials. The highest values were achieved in areas with high thermal capacity materials such as asphalt and granite and no shading. Without the cooling effect of the shade and the moisture released from vegetation, the surfaces of the squares store the heat from solar radiation. This results in higher temperatures during the evening, reaching 57.3 °C in SJS at 18:00 and 55 °C in CBS at 13:00. The lowest points are 36.3 °C in SJS and 30.2 °C in CBS.

The MRT was calculated using the monitored globe temperature standard ISO 7726:2021 [11]. In SJS, the MRT values range from 36.9 °C to 44.2 °C across the nine points, showing a variance in thermal conditions within the square. Points that were located under direct solar radiation or surrounded by surfaces with materials that absorb and emit more heat exhibited higher MRT values than the other points in the shade. In CBS, the MRT in the ten points was in a range of 31.8–49.0 °C, which indicates considerable differences in thermal states within the square, again linked to areas receiving direct solar radiation. In this square, the difference between the points is higher, mostly due to the greater presence of vegetation, which ensures shade for a larger area of the surface, reducing the MRT. The areas with higher MRT values may induce increased thermal discomfort for individuals in these locations due to higher radiant heat emissions from the surrounding surfaces. This discomfort is calculated based on the measurements of the UTCI. In SJS, the UTCI was in a range of 37.58–41.58 °C, while the range in CBS was 25.2–38.17 °C. SJS tends to display

higher UTCI values than CBS, indicating warmer perceived temperatures. The values correlate with the MRT, indicating the high impact of this parameter on thermal comfort.

Calibration of the Simulations

The results of the statistical parameters calculated using monitoring and simulation data show a satisfactory accuracy level for these simulation results. The CV(RMSE) values fall below 30%, as shown in Table 6. It should also be noted that the RMSE, which quantifies the deviation between observed and simulated data, should ideally be close to zero. In this study, the RMSE and NMBE exhibit relatively high values, probably due to inaccuracies arising from the monitoring process or limitations in the simulation model.

Table 6. Statistical parameters for the simulations' accuracy.

		NMBE	MAPE	RMSE	CV(RMSE)
AT	SJS	15%	12%	5.4	14%
	CBS	17%	13%	5.0	16%
RH	SJS	0%	0%	1.1	5%
	CBS	−3.90%	−3%	2.7	8%
MRT	SJS	17.3%	14%	6.4	16%
	CBS	3.80%	3%	4.1	12%
UTCI	SJS	19.7%	16%	9.8	25%
	CBS	−8.10%	−9%	5.3	17%

The RH values show higher accuracy than the UTCI values. Notably, the largest discrepancy in accuracy between the two squares is observed in the MRT values. CBS specifically yields significantly more accurate results than SJS, suggesting that the software performs better in shaded environments. This is the most pronounced difference between the two squares.

Any discrepancies between monitored and simulated data may arise from several factors. Firstly, the accuracy of the monitoring instruments may be compromised under extreme heat conditions, particularly when measurements are taken in direct sunlight. Additionally, previous studies [66,67] have reported discrepancies in ENVI-met simulations, often due to a lack of detailed local data on the boundary conditions or inherent modeling limitations within the software. Nevertheless, the methodology employed in this study highlights ENVI-met as a promising tool for analyzing, such as implementing vegetation or cooling materials in urban spaces commonly found in European city centers.

3.2. Simulation Results

This section includes the simulation results of the CSs of the squares as well as the MSs proposed to analyze thermal comfort for 23 July. In addition to the maps displaying the UTCI values for SJS and CBS at four different time points—6:00, 12:00, 16:00, and 22:00—hourly maps of the main climatic variables affecting thermal comfort are also included.

3.2.1. SJS-CS

Figure 10 shows the UTCI results for SJS. In this square, at 6:00, the UTCI is below 21.50 °C on the western sector and 21.5–24 °C on the square's eastern side. By noon, the UTCI substantially increases to between 34 °C and 39 °C, except for the area under the shade of the tree, where the UTCI values are in the range of 31.5–36.5 °C. At 16:00, the square area is above 41.5 °C. By 22:00, the UTCI decreases to 29–31.5 °C, and moderate heat stress is reached in the square once more.

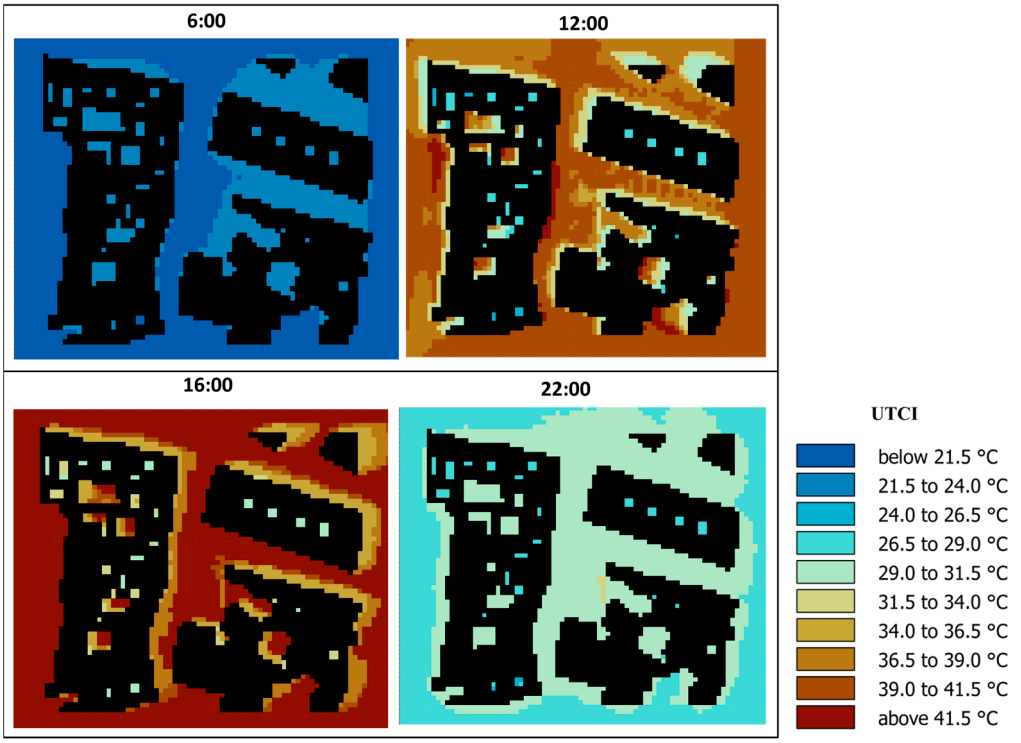

Figure 10. The UTCI results of SJS-CSCS in selected hours.

Figure 11 provides a comprehensive overview of the AT, RH, UTCI, and MRT variations at the five points selected in SJS-CS over a 24 h period. In this square, the AT rises steadily from early morning, peaking between 15:00 and 17:00 at 36 °C before it starts to decline. Points 1 and 2 generally exhibit the lowest AT at night and higher ATs in the morning. All points experience significant heat in the afternoon. While slight variations are observed in the measurement points, the overall trend suggests a similar temperature pattern across the square, with maximum variations of around 0.5 °C. This indicates a relatively uniform climate within the area.

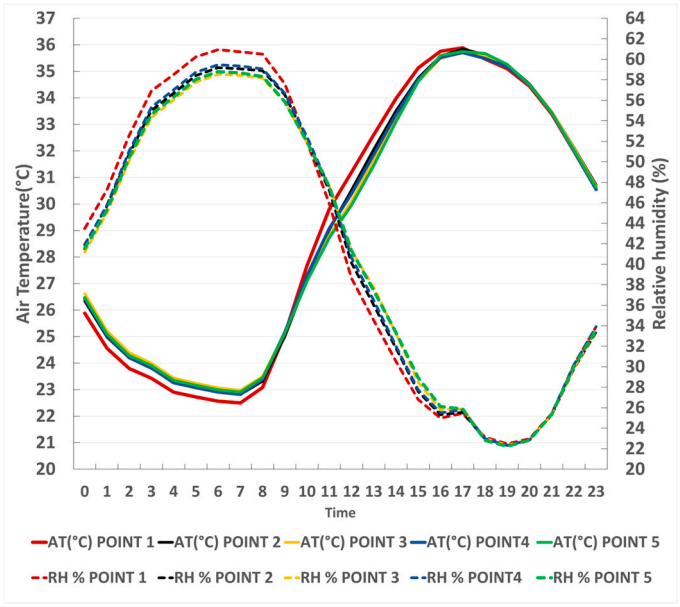

(**a**) Air temperature and relative humidity

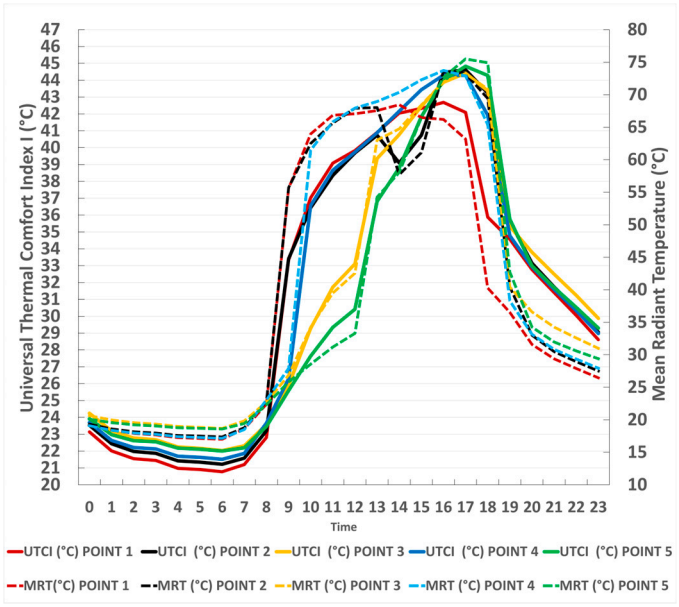

(**b**) MRT and UTCI

Figure 11. Simulation hourly results at the selected points in SJS-CSCS.

Another factor affecting thermal comfort is RH. According to Figure 11a, the RH in SJS-CS gradually increases at night (from midnight to 7:00 h), peaking at around 6:00 (between 58.0% and 60.9%) across all points. This increase is followed by a sharp decline throughout the day, reaching the lowest levels in the afternoon, between 14:00 and 17:00 (from 22.2% to 28.9%). After 18:00, the RH levels rise again, stabilizing at higher values in the late evening hours. This pattern is directly linked to the AT, which increases the RH if the temperature decreases.

WS is another influential factor impacting thermal comfort. However, vegetation and built structures in SJS hinder the wind flow across various locations, leading to speeds of less than 1 m/s. As a result, this is not considered a significant variable in this case study.

Figure 11b displays the hourly MRT and UTCI results. During the early hours (midnight to 06:00), all five points have closely grouped the MRT in the range of 17–20 °C. As the day progresses, the MRT increases significantly, especially between 09:00 and 17:00, with the MRT peaking at around 14:00 at point 4 (70.4 °C) and point 5 (75.5 °C at 17:00). Points 1 and 2 exhibit very high values earlier (around 09:00–11:00), possibly due to direct sunlight or reflective surfaces. The evening shows a cooling pattern, with the MRT dropping to below 30 °C at all points after 19:00. The differences in MRT values at midday suggest that point 4 and point 5 may well be more exposed to solar radiation or heat-retentive surfaces than the other points.

The results for the UTCI are directly related to the MRT, with the nighttime values (00:00–06:00) being also relatively uniform across the points, ranging from 20.8 °C to 24.2 °C, indicating comfortable thermal conditions. Between 09:00 and 17:00, the UTCI rises dramatically, first at points 1 and 2, exceeding 40 °C around midday, indicating thermal stress. Points 4 and 5 also show elevated values, peaking at above 44 °C in the afternoon, with point 5 reaching the highest value of 44.8 °C at 17:00. Points 3, 4, and 5 exhibit a more moderate increase than points 1 and 2, particularly in the early morning and late afternoon. These differences are directly related to solar radiation and orientation. After 18:00, the temperatures decreased steadily, returning to comfortable levels of 30–35 °C by the evening. However, the UTCI, which is also affected by the other parameters, decreases slower than the MRT, while the AT remains very high in the afternoon hours.

3.2.2. SJS-MS

This section shows the results of the proposed MS in SJS. Given the lack of shading and vegetation, canopies and a green wall are suggested, also improving the area aesthetically. In some areas, the surface material of the squares has also been changed into paved grass, reducing the thermal capacity of the existing hard pavement. These results are shown in the maps displaying the absolute differences in the AT, RH, MRT, and UTCI values at four different times (6:00 in the morning, 12:00 noon, 16:00, and 22:00) (Figure 12). Reductions in the SJS-MS values compared to SJS-CS appear in green, while red is used to indicate higher values. Based on Figure 12a, the AT absolute difference suggests that the MS in SJS has a small impact on the AT. At 6:00, the difference on the northeastern side of the square is 0.1–0.4 °C. By noon, the canopies start showing improvements, reducing the AT by 0.1 °C to 0.7 °C. In the southwest of the square, this value is from −0.2 °C to −0.5 °C, displaying a slightly increasing AT in this area. At 16:00, both canopies and the green wall provide moderate benefits, reducing temperatures by 0.1–0.4 °C. At night, the values are similar to those observed in the morning (Figure 12a).

For RH (Figure 12b), the differences are minimal and negative, which means the RH increased after implementing MSs. In the morning and at noon, these strategies increase the RH by −0.5% to −1.7%. However, by nightfall and afternoon, their influence is negligible

again (−0.5% to −0.8%). This means that although the green wall increases the RH, the effect can be considered minimal.

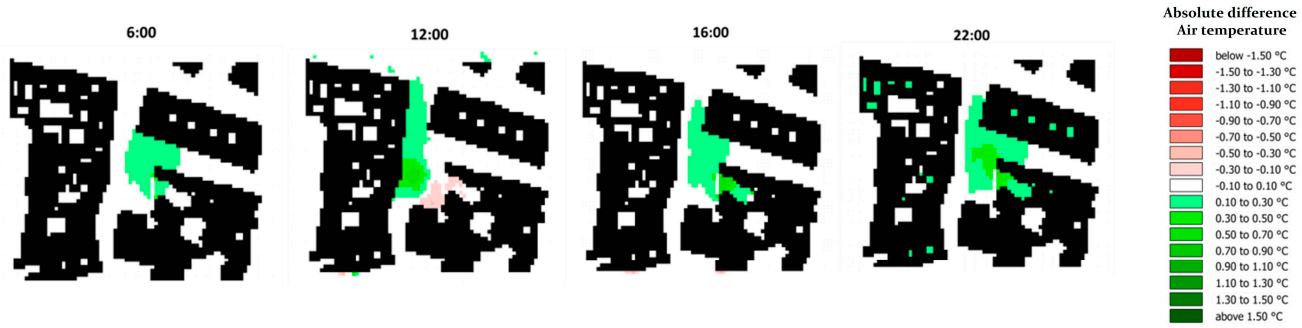

(**a**) Absolute difference in AT at four selected hours

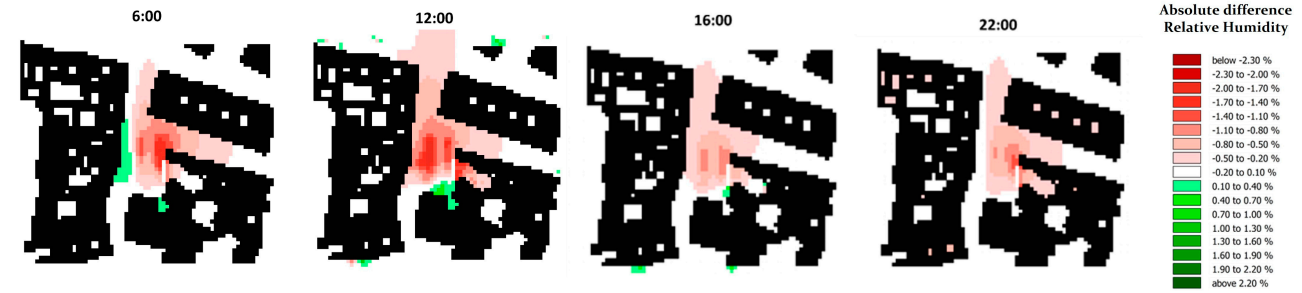

(**b**) Absolute difference in RH in four selected hours

(**c**) Absolute difference in MRT in four selected hours

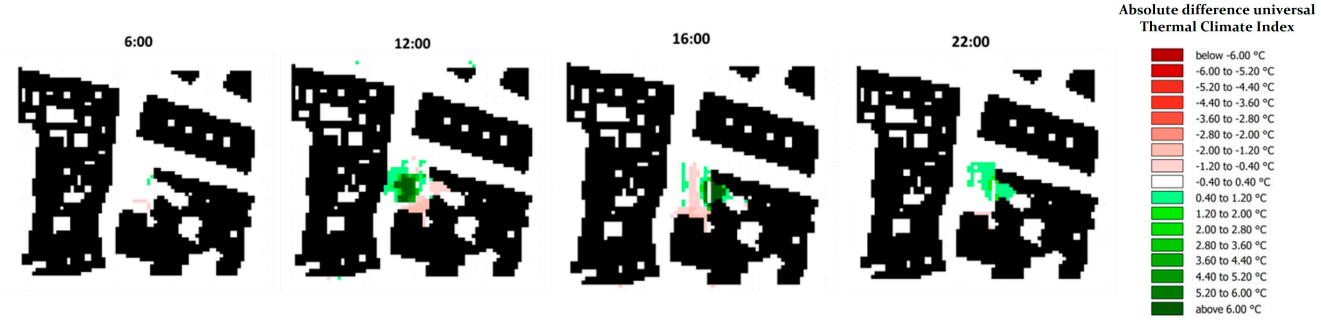

(**d**) Absolute difference in UTCI in four selected hours

Figure 12. The absolute difference in climatic variables of the mitigation scenario at four selected hours.

In terms of the MRT (Figure 12c), in the morning, the MRT differences are negative, between −0.8 °C and −3.7 °C, in the south of SJS. At noon, canopies significantly reduce the MRT by up to 22.4–29.2 °C, while the green wall provides moderate cooling in the range of 2.1–5 °C. During the afternoon, the area experiences a relatively higher MRT, with a difference of −0.8 °C to −3.7 °C, while around the green wall, the MRT difference is in a range of 2.1–5 °C, and the effect is therefore positive. At 22:00, the difference close to the

green wall is 2.1–7.9 °C. These results suggest that blocking direct sunlight using canopies is the most effective strategy, especially in the morning.

Based on the absolute difference in the UTCI in SJS shown in Figure 12d, it can be stated that the UTCI differences are minimal in the morning due to naturally cooler temperatures. By noon, canopies significantly reduce the UTCI by up to 5–6.5 °C, reducing heat stress, while the green wall provides slightly higher values, from 0.4 °C to 1.2 °C. In the afternoon and at night, the impact ranges from −1.2 °C to 2 °C.

3.2.3. CBS-CS

The results of the simulation for CBS-CS are presented in this section. As shown in Figure 13, at 8:00, the UTCI is below 22.5 °C throughout the square. By noon, it rises significantly and is between 37.5 °C and 40 °C, and the values under trees range from 32 °C to 35 °C. At 16:00, the west side displays UTCI ranges from 35 °C to 37.5 °C, while the eastern side and the center of the square show values above 42.5 °C, and the values under trees are in the range of 37.5–40 °C. By 22:00, the UTCI drops to a range of 27.5–32.5 °C.

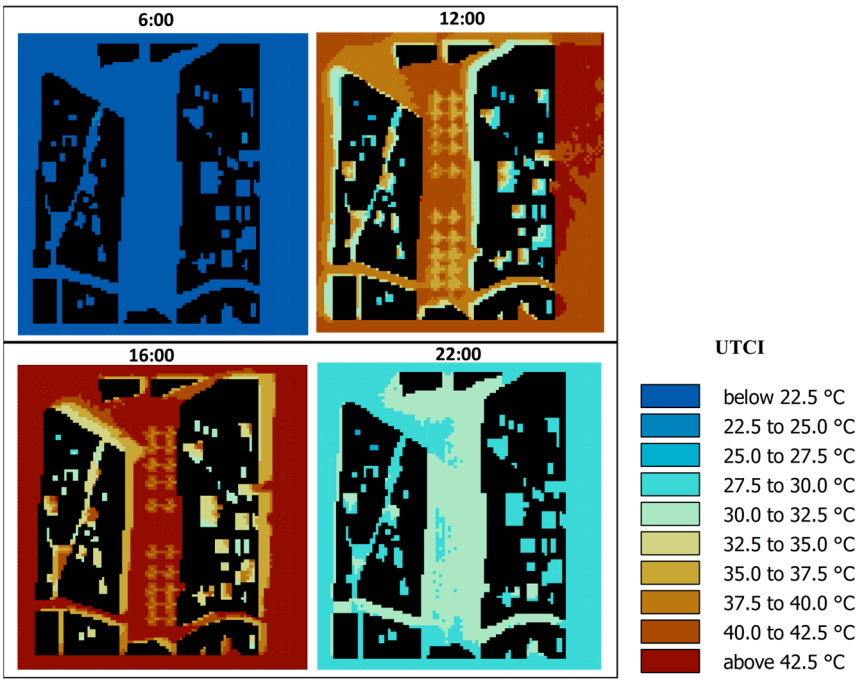

Figure 13. The UTCI results of CBS in the selected hours.

Figure 14a provides a comprehensive overview of the AT variations at the five points in the CBS-CS over 24 h. The AT analysis of this square shows that point 5 experienced the highest temperatures, peaking at 36.8 °C, probably due to greater sun exposure. Points 1 and 2 follow similar, slightly lower patterns, while points 3 and 4 consistently record the coolest temperatures, suggesting possible shading or cooling effects. These variations identify point 5 as a priority area for thermal comfort interventions. Furthermore, in contrast to the SJS-CS square, differences between points are higher throughout the day, reaching 1.5 °C at some hours.

The RH values (Figure 14a) are also in keeping with those seen in SJS-CS. These tend to be high in the early morning and decrease in the hotter midday due to the increase in temperature. In contrast to SJS-CS, this square shows more noticeable RH differences between the points selected, probably due to the higher presence of vegetation.

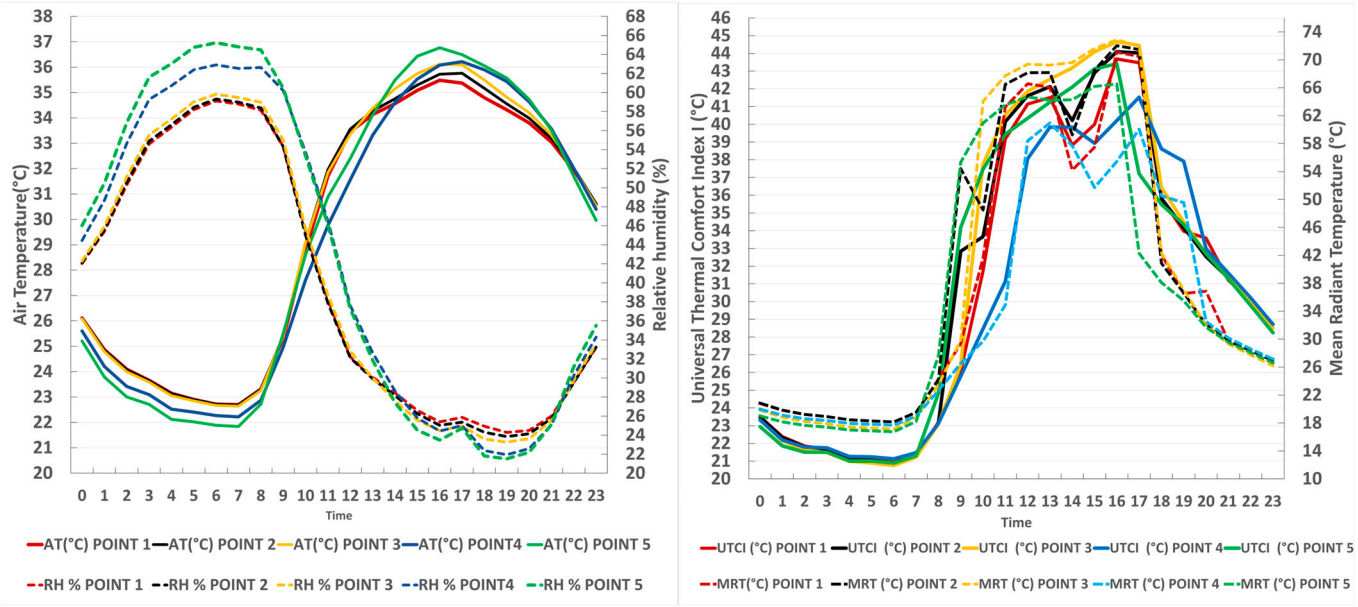

(**a**) Air temperature and Relative Humidity (**b**) MRT and UTCI

Figure 14. Simulation of hourly MRT and UTCI results at the selected points in CBS-CS.

The MRT data for CBS-CS (Figure 14b) reveal considerable variations across different points and times of the day. The MRT values during the morning hours of the day between 00:00 and 06:00 were low, remaining practically the same between points, showing varied values within the range of 16.7–20.9 °C as a reflection of the nighttime temperature. The values keep rising progressively throughout the day, starting at 09:00 and peaking from 15:00 to 17:00. At 16:00, point 3 recorded the highest MRT of the study, 72.9 °C, showing highly exposed surfaces to the sun. By evening, the square heads towards a cooling trend whose level is assumed to gradually pull down the MRT below 30 °C by night around 21:00. The continuous variations in the MRT during the sunny hours suggest that vegetation helps to reduce the MRT when it blocks the sun. However, the lack of a homogeneous canopy prevents the MRT from remaining low.

Finally, the UTCI results for CBS-CS are relatively uniform, between 00:00 and 06:00, with a range of 20.9–23.5 °C, which is considered comfortable at all points. However, there are very high discrepancies during the day. In detail, the UTCI values rise noticeably after 09:00 and reach high levels—over 40 °C, indicating high thermal stress—around midday at point 3 and the nearby point 2. Point 5 also recorded high UTCI values, peaking above 43 °C in the afternoon. Such high values indicate that these points are more exposed to direct sunlight or less sheltered from heat sources. Points 1 and 4 illustrate moderate rises in the UTCI as opposed to point 2 and point 3. After 18:00, the UTCI values decrease and return to more comfortable levels, ranging from 28 °C to 35 °C in the evening.

3.2.4. CBS-MS

According to the assessment conducted previously for CBS-CS, it is clear that improvements are required for the points exposed to the sun. In addition, the overall high UTCI values in the morning and afternoon hours prompt us to implement strategies that could increase thermal comfort. Thus, the use of different pavement materials is suggested in order to complement the canopies installed in sunny areas and the extensive presence of vegetation already found in the square. Following an iterative process for the selection of materials, the best performance was observed with the use of paved grass, a hard pavement incorporating grass and soil. The results of the strategy are shown in this section.

At 6:00, differences in the AT are quite small, ranging from 0.3 °C to 1.1 °C, showing that the effect in the early morning is minimal. At noon, cooling is more noticeable in the north and center sections, with values of between 1.5 °C and 2.7 °C and values of between 0.3 °C and 0.7 °C on the southern side, showing effective cooling from paved grass and canopies. At 16:00, the cooling effects are reduced, with differences in a range of 0.3–1.5 °C. By 22:00, the AT differences drop in the range of 0.3 °C to 0.7 °C (Figure 15a).

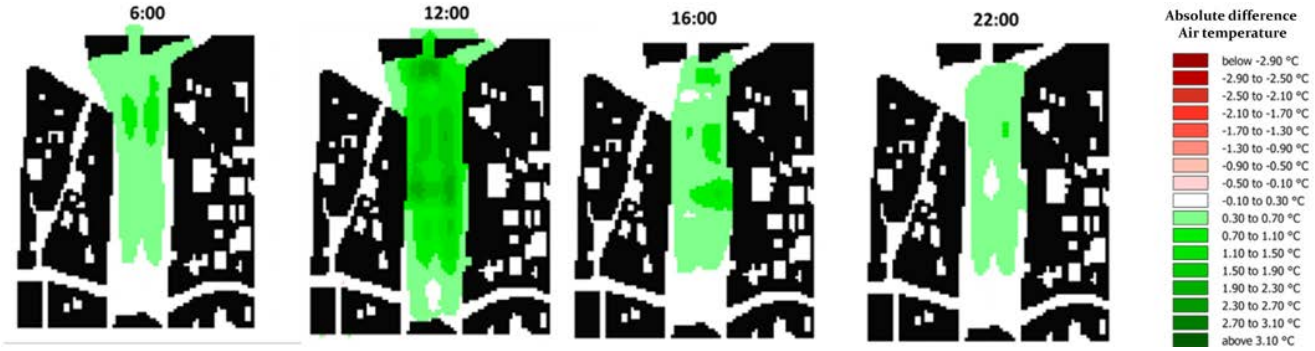

(**a**) Absolute difference in AT at four selected hours

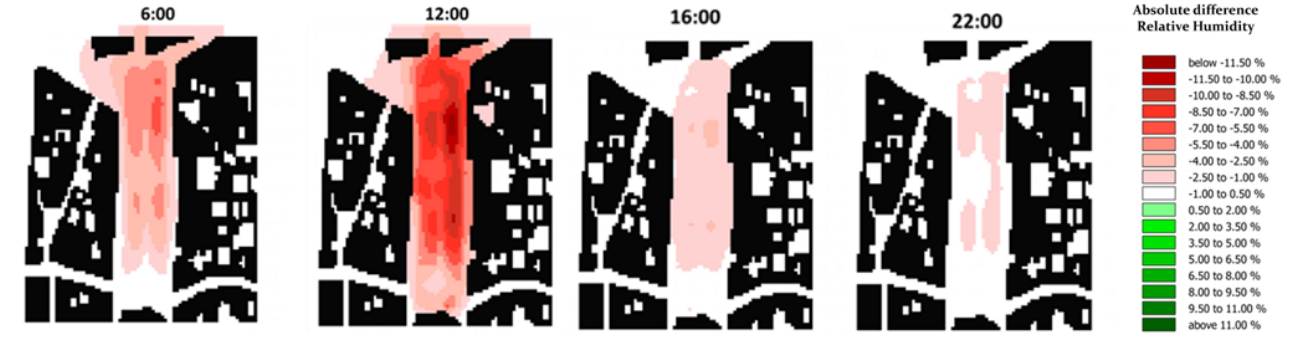

(**b**) Absolute difference in RH in four selected hours

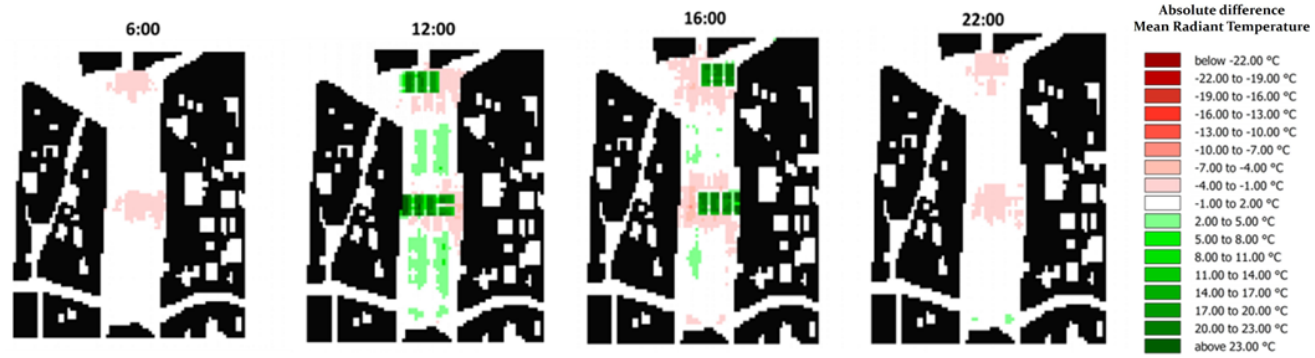

(**c**) Absolute difference in MRT in four selected hours

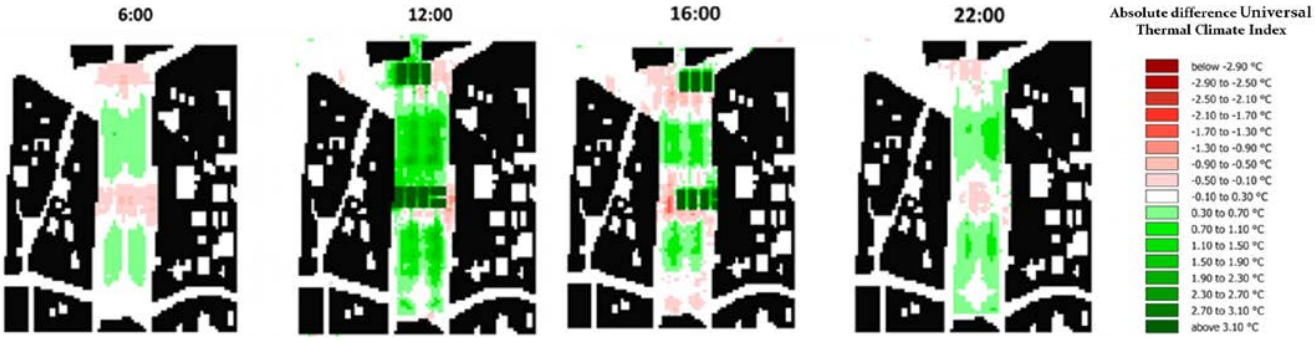

(**d**) Absolute difference in UTCI in four selected hours

Figure 15. The absolute difference in climatic variables of the CBS mitigation scenario at four selected hours.

The absolute difference in RH is negative at all hours in the area. This shows that the mitigation strategy has increased the RH by noon, from −4% to −10%, especially in the central and paved areas, suggesting a possible increase in evaporation or reduction in moisture retention due to the effects of the MSs. In the afternoon, at 16:00, the RH differences are lower than in the morning, found in the range of −1.00% to −2.5%, while during the night, at 22:00, the level is relatively stable, and only a few changes from 0.5% to −2.5% were recorded, indicating that, during the night, the effect of the MSs on RH are lessened (Figure 15b).

In terms of the MRT, in the early morning, the absolute difference is very low and negative, between −1 °C and −4 °C under the canopies in the north and center sections of CBS. At noon and afternoon (12:00, 16:00), these values increase by 2 °C to 5 °C in the paved grass area and 14 °C to 23 °C under the canopies. However, by 22:00, the differences in the MRT are similar to those in the early morning (Figure 15c).

The absolute difference in the UTCI in CBS, as shown in Figure 15d, indicates that, in the morning, these values are between −0.5 °C and −0.1 °C under the canopies and 0.3–0.7 °C for paved grass. At 12:00 and 16:00, they range from 1.1 °C to 2.3 °C under the vegetation and above 3.1 °C under the canopies. At night, this value is similar to the morning values.

4. Discussion

The selection of these two case studies in the historic center of Seville responds to the aim of analyzing two different conceptions of an urban square: from very small ones, generally hard paved and lacking other elements, to medium-sized ones with vegetation. Both case studies exemplify one of the most characteristic elements of the historic center of Seville and other regional cities. Small plazas, understood as expansions and widenings within a dense and narrow urban fabric, function as public spaces for social gathering and interaction among residents while also aiming to provide comfortable areas. As the results have shown, their climatic performance is strongly influenced not only by their urban structure but also by the use of traditional construction materials on pavements and adjacent buildings. The findings discussed here can be easily extrapolated to other examples with similar characteristics within the city or region.

4.1. Regarding the Monitoring and Validation of the Study

Monitoring results were used to calibrate the simulations. The error results obtained in this section fall within the acceptable range, as reported in the literature. However, it should be noted that there is no established standard for this type of outdoor simulation. Thus, a standard commonly used in energy simulations was adopted as a reference.

Another possible way to validate the values obtained is through comparisons with previous studies. While validation with monitored data is not always available in the literature, several previous studies have analyzed the MSs and validated simulations of the MRT (showing the poorest results) reaching 7 °C [68] and 11.2 °C [69], thus confirming that this study can also be validated with the data obtained. However, it is essential to take potential inaccuracies into account, as the results of this study are significant for trends, regardless of the absolute values.

4.2. Regarding the Effectiveness of the Strategies Proposed

The simulation of the CS of both squares showed that, for all the parameters analyzed, the variations were higher in CBS than in SJS. There are two reasons for this. Firstly, SJS is much smaller in size, limiting different environments inside the square. In addition, the large number of trees in CBS produces changes in solar radiation and humidity patterns

that directly affect the AT, affecting the UTCI. Although the comfort values are high in the late morning and the afternoon in both squares, the variability of the MRT in CBS increases the comfort conditions since people can choose what part of the broader area they prefer to occupy. The current use of the squares validates this statement, as CBS is much more livable than SJS, even in extremely hot conditions. This is in keeping with previous studies [54], which demonstrated the high local cooling potential of small vegetation spaces or urban parks, providing climate-cooling areas for shelter.

After applying the MSs to improve thermal comfort in hours of extreme heat, the results prove that the most effective strategy in both squares is the installation of canopies, with reductions in the UTCI of up to 6.5 °C in SJS and 5 °C in CBS. Shading elements, such as pergolas or canopies, reduce direct solar radiation on surfaces and people, improving thermal comfort. Previous research also indicates that shading can decrease the MRT by up to 20–30 °C [70]. However, these improvements are limited almost exclusively to directly shaded areas, thus limiting the strategy's effectiveness to certain hours. In addition, the results suggest that the canopies could reduce night heat release and cause a slight reduction in the thermal comfort observed during the night. This conclusion further supports previous studies in the same field [4], which identified removable canopies as the best option, even though it is not yet possible to simulate dynamic shading in ENVI-met. According to the existing literature [4,46], these results and the reduction reached in the UTCI are generally to be expected, as similar reductions have been obtained in these and other studies [38], which reached even higher temperature reductions.

Trees and greenery can significantly reduce surface and ATs through shading and evapotranspiration, both on a small scale and on a larger urban scale, as seen in previous studies [55]. Meanwhile, other studies have shown that increasing vegetation cover by 10–20% can lower ambient temperatures by 2–3 °C [71,72]. However, strategies for vegetation and water use are very limited in the existing areas. In fact, their use is ruled out in these areas due to the climate change projections of lower precipitations. In CBS, where vegetation was already substantial, this strategy was not even proposed, as it could worsen comfort due to an increased RH, as demonstrated by [4]. Given the area's protected heritage status and limited space, it is not possible to add new trees in SJS. The green wall was therefore proposed as an alternative. However, its microclimatic effect was significantly reduced, and while this strategy can be considered to improve comfort perception for the most part, it produces no essential measurable benefits in terms of temperature.

It was challenging to optimize the strategy of improving the material of the ground surface. According to the existing literature [43], high-albedo pavements and coatings reflect more solar radiation, reducing the ST. In fact, studies report a ST reduction of 5–10 °C when cooling materials are applied in existing urban spaces, as proved previously [73]. However, in this type of square, previous simulation results with higher albedo in this study consistently reduced thermal comfort. This was caused by an increased MRT due to the reflected radiation. The proximity of reflecting surfaces due to the geometry of these spaces makes high-albedo material preferably avoidable. Previous studies on the consequences of albedo in confined spaces further support this conclusion [44]. For this reason, rather than changing the albedo, the strategy in this study was to reduce the heat captured by hard materials, an approach that has proved very beneficial to comfort reduction in previous studies [53]. The paved grass proposed absorbs much less heat than existing materials. Although the reduction in the UTCI was only a few degrees, the effect is more homogeneous in the area of the square and improves comfort, even in shaded areas.

4.3. Limitations

This study is limited to the two case studies analyzed, although the conclusions can be extrapolated to similar spaces in many cities worldwide with similar structures and climates. Other limitations inherent to the methodology were also carefully considered during this analysis. ENVI-met simulations are constrained by their static representation of dynamic shading effects and cannot account for long-term temporal variability. Additionally, instrument accuracy under extreme heat conditions may introduce minor discrepancies. Despite these limitations, the combined use of field data, model calibration, and simulations provide a robust framework for understanding and mitigating urban thermal discomfort in heritage contexts.

The results are also limited by the software used, which can only simulate traditionally used materials with static characteristics. Future work should focus on analyzing the potential of newer technologically advanced materials, such as supercool materials, which may be the future regarding increasing the effectiveness of MSs under extreme climate projections, as suggested in previous studies [57]. However, new tools must still be developed to include these characteristics in the analysis.

5. Conclusions

This study highlights the critical importance of addressing thermal comfort in urban squares, particularly in historic neighborhoods such as the Casco Antiguo of Seville, where the effects of the UHI phenomenon are exacerbated by the lack of vegetation, shading, and water features, typical urban characteristics of the traditional historical urban fabric in old cities. The comparative analysis of SJS and CBS through in-person monitoring and simulation methods highlights the complex interplay of traditional urban design elements, constructive material properties, and microclimatic conditions generated by historic urban textures, which can be detrimental to comfort effects under warm conditions, as shown in this study.

The findings reveal that SJS experiences significantly higher thermal stress due to its limited greenery and shading, with the UTCI values peaking at over 44 °C at midday. In contrast, CBS benefits from better vegetation coverage, leading to lower UTCI values and enhanced thermal comfort in shaded areas. Nevertheless, CBS recorded the highest MRT in the study, 72.9 °C, showing surfaces highly exposed to the sun. These differences emphasize the pivotal role of urban vegetation and shading in moderating thermal conditions.

This study's simulation results provide actionable insights into effective MSs for improving thermal comfort in both squares:

- Canopies emerged as the most impactful intervention, significantly reducing the UTCI values (by up to 6.5 °C in SJS and 5 °C in CBS) during peak hours by providing extensive shading.
- Green walls offered localized cooling effects, lowering the MRT by up to 5 °C while enhancing the aesthetic and ecological values.
- Paved grass and permeable asphalt demonstrated moderate cooling effects, reducing surface and ATs in heavily exposed and already shaded areas.

These findings validate the strategies proposed, highlighting their adaptability to historic urban environments.

By implementing these solutions, city planners can achieve a balance between preserving the cultural heritage of historic squares and enhancing their climate resilience. Moreover, this research provides valuable guidance for integrating thermal comfort improvements into urban design, offering a replicable framework for other cities grappling with the challenges of UHI and thermal discomfort. This study reinforces the need for targeted, evidence-based interventions to mitigate heat stress in urban squares, ensuring

that these vital public spaces remain functional, sustainable, and enjoyable for residents and visitors alike. By adopting a holistic approach that combines green infrastructure, shading elements, and innovative materials, cities can enhance thermal comfort while preserving their historical and cultural integrity.

Thus, policymakers are encouraged to integrate thermal comfort considerations into urban planning regulations, particularly for historic districts. This includes the promotion of adaptive shading structures and green infrastructure to mitigate UHI effects while preserving cultural heritage. Guidelines for urban conservation projects should incorporate climate-resilient designs, such as permeable pavements and vegetation, as standard practices. In contrast, industry stakeholders, particularly in the field of architecture and construction, are advised to innovate with materials and designs that enhance thermal performance while aligning with heritage preservation principles. A clear example of this can be found in lightweight, modular shading solutions and high/medium-albedo materials suitable for historic settings, which are critical areas for development. Collaboration between heritage conservationists and green technology developers can lead to scalable solutions for sustainable urban regeneration.

Finally, future studies should explore the long-term performance of MSs under changing climate conditions, incorporating dynamic simulations that take seasonal variations into consideration. Expanding the study to include different urban forms and climates could validate these findings and provide transferable solutions for other heritage cities. Investigating comfort and the socio-economic impacts of thermal mitigation measures, such as community engagement and cost-benefit analysis, could offer deeper insights for practical implementation.

Author Contributions: Conceptualization, V.P.L.-C. and C.G.-M.; Data curation, P.R. and J.S.-C.; Formal analysis, P.R.; Funding acquisition, C.G.-M.; Investigation, P.R. and J.S.-C.; Methodology, V.P.L.-C. and C.G.-M.; Project administration, C.G.-M.; Resources, C.G.-M.; Software, P.R., V.P.L.-C. and J.S.-C.; Supervision, V.P.L.-C. and C.G.-M.; Validation, V.P.L.-C.; Visualization, P.R.; Writing—original draft, P.R. and V.P.L.-C.; Writing—review and editing, V.P.L.-C., J.S.-C. and C.G.-M. All authors have read and agreed to the published version of the manuscript.

Funding: This work has been supported by the project PID2021-124539OB-I00 funded by MCIN/AEI/10.13039/501100011033 and by "ERDF A way of making Europe", project TED2021-129347B-C21 funded by MCIN/AEI/10.13039/501100011033 and by the "European Union NextGenerationEU/PRTR". The Ministerio de Ciencia, Innovación y Universidades supported a predoctoral contract granted to J.S.-C. (FPU21/02458), and a Juan de la Cierva Postdoctoral Fellowship was granted to V.P.L.-C. (JDC2023-050880-I).

Data Availability Statement: The authors will make the raw data supporting this article's conclusions available upon request.

Conflicts of Interest: The authors declare no conflicts of interest.

References

1. United Nations, Department of Economic and Social Affairs, Population Division. *World Urbanization Prospects The 2018 Revision (ST/ESA/SER.A/420)*; United Nations: New York, NY, USA, 2019.
2. Salih, K.; Nagy, I.R.B. Review of the Role of Urban Green Infrastructure on Climate Resiliency: A Focus on Heat Mitigation Modelling Scenario on the Microclimate and Building Scale. *Urban Sci.* **2024**, *8*, 220. [CrossRef]
3. Yilmaz, D.; Ozturk, S. Urban Heat Island From A 3d Modeling Perspective—A Review. *Environ. Model. Assess.* **2024**, *29*, 1111–1129. [CrossRef]
4. Sola-Caraballo, J.; Lopez-Cabeza, V.P.; Roa-Fernández, J.; Rivera-Gomez, C.; Galan-Marin, C. Assessing and upgrading urban thermal resilience of a Spanish MoMo neighbourhood over the span of 1960–2080. *Build. Environ.* **2024**, *256*, 111485. [CrossRef]
5. Chu, Z.; Li, S.; Li, T.; Qian, H.; Liu, C.; Yan, Z. Numerical simulation of layout and landscape elements on the thermal environment of urban squares. *Ecol. Inform.* **2024**, *82*, 102770. [CrossRef]

6. Gonçalves, A.; Ribeiro, A.C.; Maia, F.; Nunes, L.; Feliciano, M. Influence of green spaces on outdoors thermal comfort-structured experiment in a Mediterranean climate. *Climate* **2019**, *7*, 20. [CrossRef]
7. Aghamolaei, R.; Azizi, M.M.; Aminzadeh, B.; O'donnell, J. A comprehensive review of outdoor thermal comfort in urban areas: Effective parameters and approaches. *Energy Environ.* **2023**, *34*, 2204–2227. [CrossRef]
8. Maruani, T.; Amit-Cohen, I. Open space planning models: A review of approaches and methods. *Landsc. Urban Plan.* **2007**, *81*, 1–13. [CrossRef]
9. Chen, L.; Ng, E. Outdoor thermal comfort and outdoor activities: A review of research in the past decade. *Cities* **2012**, *29*, 118–125. [CrossRef]
10. Mandić, L.; Đukić, A.; Marić, J.; Mitrović, B. A Systematic Review of Outdoor Thermal Comfort Studies for the Urban (Re)Design of City Squares. *Sustainability* **2024**, *16*, 4920. [CrossRef]
11. Zhang, J.; Zhang, F.; Jiang, L.; Guo, W.; Cao, Q.; Shi, M.; Xiao, A. Comparative review of urban geometric parameters and their uses in outdoor thermal environment studies. *J. Urban Manag.* **2024**, *13*, 541–552. [CrossRef]
12. Tan, Y.; Li, C.; Feng, H.; Yang, J. Exploring the Land Cover Material Interaction of Urban Open Space on the Thermal Comfort of Crowds in High-Temperature Environments and Retrofit Strategies: Two Case Studies in the Nanjing Xinjiekou District. *Land* **2024**, *13*, 314. [CrossRef]
13. da Silva, P.W.S.; Duarte, D.H.S.; Rahman, M.A.; Rötzer, T.; Pauleit, S. Testing Strategies for Planting Design in Urban Squares to Improve Human Comfort throughout the Seasons. *Atmosphere* **2024**, *15*, 870. [CrossRef]
14. Banerjee, S.; Pek, R.X.Y.; Yik, S.K.; Ny Ching, G.; Ho, X.T.; Dzyuban, Y.; Crank, P.J.; Acero, J.A.; Chow, W.T. Assessing impact of urban densification on outdoor microclimate and thermal comfort using ENVI-met simulations for Combined Spatial-Climatic Design (CSCD) approach. *Sustain. Cities Soc.* **2024**, *105*, 105302. [CrossRef]
15. Pistore, L.; Pasut, W. Roots and Mechanisms of Thermal Comfort Expectations: From Individuals' Own Background to Adaptation and Change. In *Proceedings of the 5th International Conference on Building Energy and Environment*; Wang, L.L., Ge, H., Zhai, Z.J., Qi, D., Ouf, M., Sun, C., Wang, D., Eds.; Springer Nature: Singapore, 2023; pp. 2325–2336.
16. Lenzuni, P.; Freda, D.; Del Gaudio, M. Classification of thermal environments for comfort assessment. *Ann. Occup. Hyg.* **2009**, *53*, 325–332. [CrossRef] [PubMed]
17. Ahmed, N.M.; Altamura, P.; Giampaoletti, M.; Hemeida, F.A.; Mohamed, A.F.A. Optimizing human thermal comfort and mitigating the urban heat island effect on public open spaces in Rome, Italy through sustainable design strategies. *Sci. Rep.* **2024**, *14*, 19931. [CrossRef] [PubMed]
18. Njoku, C.A.; Daramola, M.T. Human Outdoor Thermal Comfort Assessment in a Tropical Region: A Case Study. *Earth Syst. Environ.* **2019**, *3*, 29–42. [CrossRef]
19. Błażejczyk, K. UTCI—10 years of applications. *Int. J. Biometeorol.* **2021**, *65*, 1461–1462. [CrossRef]
20. Brecht, B.M.; Schädler, G.; Schipper, J.W. UTCI climatology and its future change in Germany—An RCM ensemble approach. *Meteorol. Z.* **2020**, *29*, 97–116. [CrossRef]
21. UTCI—Universal Thermal Climate Index. n.d. Available online: http://www.utci.org/ (accessed on 3 June 2020).
22. Jendritzky, G.; de Dear, R.; Havenith, G. UTCI—Why another thermal index? *Int. J. Biometeorol.* **2012**, *56*, 421–428. [CrossRef]
23. Krüger, E.L. Literature Review on UTCI Applications. In *Applications of the Universal Thermal Climate Index UTCI in Biometeorology: Latest Developments and Case Studies*; Krüger, E.L., Ed.; Springer International Publishing: Cham, Switzerland, 2021; pp. 23–65. [CrossRef]
24. Lee, H.; Park, S.; Mayer, H. Approach for the vertical wind speed profile implemented in the UTCI basics blocks UTCI applications at the urban pedestrian level. *Int. J. Biometeorol.* **2024**, 1–14. [CrossRef] [PubMed]
25. Feng, L.; Yang, S.; Zhou, Y.; Sun, J. Optimization strategy of architectural forms to improve the thermal comfort of residential area. *J. Build. Eng.* **2024**, *86*, 108905. [CrossRef]
26. Li, Y.; Zhang, Y.; Wang, Y.; Song, Z.; Zhou, Z.; Ding, L.; Chen, C.; Jin, X.; Cheng, Y. Assessing thermal comfort for the elderly in historical districts and proposing adaptive urban design strategies: A case study in Zhenjiang, China. *Landsc. Ecol. Eng.* **2024**, *21*, 29–46. [CrossRef]
27. Lin, C.; Wu, Z.; Li, H.; Huang, J.; Huang, Q. Comprehensive analysis on the thermal comfort of various greening forms: A study in hot-humid areas. *Environ. Res. Commun.* **2024**, *6*, 025010. [CrossRef]
28. Yahia, M.W.; Johansson, E.; Thorsson, S.; Lindberg, F.; Rasmussen, M.I. Effect of urban design on microclimate and thermal comfort outdoors in warm-humid Dar es Salaam, Tanzania. *Int. J. Biometeorol.* **2018**, *62*, 373–385. [CrossRef] [PubMed]
29. Coccolo, S.; Paoli, M.D.; Stracqualursi, A.; Andreucci, M.B. Design the Urban Microclimate: Nature-Based Solutions and Technology at Nexus. In *Urban Services to Ecosystems: Green Infrastructure Benefits from the Landscape to the Urban Scale*; Catalano, C., Andreucci, M.B., Guarino, R., Bretzel, F., Leone, M., Pasta, S., Eds.; Springer International Publishing: Cham, Switzerland, 2021; pp. 413–433. [CrossRef]
30. Gomaa, M.M.; El Menshawy, A.; Nabil, J.; Ragab, A. Investigating the Impact of Various Vegetation Scenarios on Outdoor Thermal Comfort in Low-Density Residential Areas of Hot Arid Regions. *Sustainability* **2024**, *16*, 3995. [CrossRef]

31. Kamata, Y.; Kang, J.E. Effect of greening vacant houses on improvement in thermal environment using ENVI-met simulation: A case study on Busan metropolitan city. *Environ. Plan. B Urban Anal. City Sci.* **2024**, *51*, 1308–1321. [CrossRef]
32. Nouri, A.S.; Costa, J.P.; Santamouris, M.; Matzarakis, A. Approaches to outdoor thermal comfort thresholds through public space design: A review. *Atmosphere* **2018**, *9*, 108. [CrossRef]
33. Ma, X.; Chau, C.; Lu, S.; Leung, T.; Li, H. Modelling the effects of neighbourhood and street geometry on pedestrian thermal comfort in Hong Kong. *Arch. Sci. Rev.* **2024**, 1–16. [CrossRef]
34. Liu, Z.; Li, J.; Xi, T. A Review of Thermal Comfort Evaluation and Improvement in Urban Outdoor Spaces. *Buildings* **2023**, *13*, 3050. [CrossRef]
35. Qi, J.; He, B.-J. Urban Heat Mitigation Strategies. In *Climate Change and Cooling Cities*; Cheshmehzangi, A., He, B.-J., Sharifi, A., Matzarakis, A., Eds.; Springer Nature: Singapore, 2023; pp. 21–44. [CrossRef]
36. Srivastava, V.T.; Sharma, A.; Jadon, S.S. A review of the formation, mitigation strategies from 50 years of global urban heat island studies. *Environ. Dev. Sustain.* **2024**. [CrossRef]
37. Irfeey, A.M.M.; Chau, H.-W.; Sumaiya, M.M.F.; Wai, C.Y.; Muttil, N.; Jamei, E. Sustainable Mitigation Strategies for Urban Heat Island Effects in Urban Areas. *Sustainability* **2023**, *15*, 10767. [CrossRef]
38. Santamouris, M.; Ding, L.; Fiorito, F.; Oldfield, P.; Osmond, P.; Paolini, R.; Prasad, D.; Synnefa, A. Passive and active cooling for the outdoor built environment—Analysis and assessment of the cooling potential of mitigation technologies using performance data from 220 large scale projects. *Sol. Energy* **2017**, *154*, 14–33. [CrossRef]
39. Santamouris, M.; Synnefa, A.; Karlessi, T. Using advanced cool materials in the urban built environment to mitigate heat islands and improve thermal comfort conditions. *Sol. Energy* **2011**, *85*, 3085–3102. [CrossRef]
40. Castellani, B.; Morini, E.; Anderini, E.; Filipponi, M.; Rossi, F. Development and characterization of retro-reflective colored tiles for advanced building skins. *Energy Build.* **2017**, *154*, 513–522. [CrossRef]
41. Zhang, R.; Xu, X.; Liu, K.; Kong, L.; Wang, W.; Wortmann, T. Airflow modelling for building design: A designers' review. *Renew. Sustain. Energy Rev.* **2024**, *197*, 114380. [CrossRef]
42. Li, Y.; Ren, C.; Ho, J.Y.-E.; Shi, Y. Landscape metrics in assessing how the configuration of urban green spaces affects their cooling effect: A systematic review of empirical studies. *Landsc. Urban Plan.* **2023**, *239*, 104842. [CrossRef]
43. Zhao, Y.; Zhao, K.; Zhang, X.; Zhang, Y.; Du, Z. Assessment of combined passive cooling strategies for improving outdoor thermal comfort in a school courtyard. *Build. Environ.* **2024**, *252*, 111247. [CrossRef]
44. Lopez-Cabeza, V.P.; Alzate-Gaviria, S.; Diz-Mellado, E.; Rivera-Gomez, C.; Galan-Marin, C. Albedo influence on the microclimate and thermal comfort of courtyards under Mediterranean hot summer climate conditions. *Sustain. Cities Soc.* **2022**, *81*, 103872. [CrossRef]
45. Lai, D.; Liu, W.; Gan, T.; Liu, K.; Chen, Q. A review of mitigating strategies to improve the thermal environment and thermal comfort in urban outdoor spaces. *Sci. Total Environ.* **2019**, *661*, 337–353. [CrossRef] [PubMed]
46. Garcia-Nevado, E.; Beckers, B.; Coch, H. Assessing the cooling effect of urban textile shading device through time-lapse thermography. *Sustain. Cities Soc.* **2020**, *63*, 102458. [CrossRef]
47. Wang, Q.; Peng, L.L.; Jiang, W.; Yin, S.; Feng, N.; Yao, L. Urban form affects the cool island effect of urban greenery via building shadows. *Build. Environ.* **2024**, *254*, 111398. [CrossRef]
48. Doulos, L.; Santamouris, M.; Livada, I. Passive cooling of outdoor urban spaces. The role of materials. *Sol. Energy* **2004**, *77*, 231–249. [CrossRef]
49. Kolokotsa, D.D.; Giannariakis, G.; Gobakis, K.; Giannarakis, G.; Synnefa, A.; Santamouris, M. Cool roofs and cool pavements application in Acharnes, Greece. *Sustain. Cities Soc.* **2018**, *37*, 466–474. [CrossRef]
50. Diz-Mellado, E.; López-Cabeza, V.P.; Rivera-Gómez, C.; Naboni, E.; Galán-Marín, C. Optimizing a courtyard microclimate with adaptable shading and evaporative cooling in a hot mediterranean climate. *J. Build. Eng.* **2024**, *88*, 109167. [CrossRef]
51. Bruse, M.; Simon, H. ENVI-Met. 2004. Available online: https://envi-met.com (accessed on 3 January 2025).
52. Faragallah, R.N.; Ragheb, R.A. Evaluation of thermal comfort and urban heat island through cool paving materials using ENVI-Met. *Ain Shams Eng. J.* **2022**, *13*, 101609. [CrossRef]
53. Sola-Caraballo, J.; Lopez-Cabeza, V.P.; Roa-Fernandez, J.; Rivera-Gomez, C.; Palomares-Figueres, M.T.; Galan-Marin, C. Assessing the microclimatic adaptation of a Modern Movement 1960s neighbourhood through its urban evolution. In Proceedings of the 18th IBPSA International Conference, Buildings Simulation 2023, Shanghai, China, 4–6 September 2023. [CrossRef]
54. Parison, S.; Chaumont, M.; Kounkou-Arnaud, R.; Long, F.; Bernik, A.; Da Silva, M.; Hendel, M. The Effects of Greening a Parking Lot as a Heat Mitigation Strategy on Outdoor Thermal Stress Using Fixed and Mobile Measurements: Case-Study Project "Tertiary Forest. *Sustain. Cities Soc.* **2023**, *98*, 104818. [CrossRef]
55. Wollschläger, N.; Zinck, F.; Schlink, U. Sustainable Urban Development for Heat Adaptation of Small and Medium Sized Communities. *Land* **2022**, *11*, 1385. [CrossRef]
56. Maiullari, D.; Gherri, B.; Finizza, C.; Maretto, M.; Naboni, E. Climate change and indoor temperature variation in Venetian buildings: The role of density and urban form. *J. Phys. Conf. Ser.* **2021**, *2042*, 012060. [CrossRef]

57. Santamouris, M.; Yun, G.Y. Recent development and research priorities on cool and super cool materials to mitigate urban heat island. *Renew. Energy* **2020**, *161*, 792–807. [CrossRef]
58. Takva, Y.; Takva, Ç.; İlerisoy, Z.Y. Sustainable Adaptive Reuse Strategy Evaluation for Cultural Heritage Buildings. *Int. J. Built Environ. Sustain.* **2023**, *10*, 25–37. [CrossRef]
59. Aguilar-Sanchez, M.; Almodovar-Melendo, J.-M.; Cabeza-Lainez, J. Thermal Performance Assessment of Burkina Faso's Housing Typologies. *Buildings* **2023**, *13*, 2719. [CrossRef]
60. Lopez-Cabeza, V.P.; Agarwal, A. Sustainable strategies for improving passive survivability of the traditional Pol House in Ahmedabad. *Build. Environ.* **2022**, *207*, 108503. [CrossRef]
61. Sola-Caraballo, J.; Serrano-Jiménez, A.; Rivera-Gomez, C.; Galan-Marin, C. Multi-Criteria Assessment of Urban Thermal Hotspots: A GIS-Based Remote Sensing Approach in a Mediterranean Climate City. *Remote Sens.* **2025**, *17*, 231. [CrossRef]
62. Gobierno de España, Agencia Estatal de Meteorología—AEMET. n.d. Available online: http://www.aemet.es/es/portada (accessed on 4 September 2023).
63. López-Cabeza, V.; Galán-Marín, C.; Rivera-Gómez, C.; Roa-Fernández, J. Courtyard microclimate ENVI-met outputs deviation from the experimental data. *Build. Environ.* **2018**, *144*, 129–141. [CrossRef]
64. Complete Guide—ENVI-Met. n.d. Available online: https://envi-met.com/tutorials-overview/ (accessed on 22 July 2024).
65. ASHRAE. ASHRAE Guideline 14-2014. Measurement of Energy, Demand, and Water Savings. 2014. Available online: https://www.ashrae.org/technical-resources/standards-and-guidelines#technology1 (accessed on 3 January 2025).
66. Pacifici, M.; Nieto-Tolosa, M. Comparing ENVI-Met and Grasshopper Modelling Strategies to Assess Local Thermal Stress and Urban Heat Island Effects. In *Urban Microclimate Modelling for Comfort and Energy Studies*; Palme, M., Salvati, A., Eds.; Springer International Publishing: Cham, Switzerland, 2021; pp. 293–316. [CrossRef]
67. Perini, K.; Chokhachian, A.; Dong, S.; Auer, T. Modeling and simulating urban outdoor comfort: Coupling ENVI-Met and TRNSYS by grasshopper. *Energy Build.* **2017**, *152*, 373–384. [CrossRef]
68. Gál, C.V.; Kántor, N. A comparative numerical simulation and validation study. *Urban Clim.* **2020**, *32*, 100571. [CrossRef]
69. Crank, P.J.; Middel, A.; Wagner, M.; Hoots, D.; Smith, M.; Brazel, A. Validation of seasonal mean radiant temperature simulations in hot arid urban climates. *Sci. Total Environ.* **2020**, *749*, 141392. [CrossRef] [PubMed]
70. Taleghani, M.; Sailor, D.; A Ban-Weiss, G. Micrometeorological simulations to predict the impacts of heat mitigation strategies on pedestrian thermal comfort in a Los Angeles neighborhood. *Environ. Res. Lett.* **2016**, *11*, 024003. [CrossRef]
71. Cohen, P.; Potchter, O.; Schnell, I. The impact of an urban park on air pollution and noise levels in the Mediterranean city of Tel-Aviv, Israel. *Environ. Pollut.* **2014**, *195*, 73–83. [CrossRef]
72. Shashua-Bar, L.; Hoffman, M.E. Vegetation as a climatic component in the design of an urban street: An empirical model for predicting the cooling effect of urban green areas with trees. *Energy Build.* **2000**, *31*, 221–235. [CrossRef]
73. Pisello, A.L.; Cotana, F. The thermal effect of an innovative cool roof on residential buildings in Italy: Results from two years of continuous monitoring. *Energy Build.* **2014**, *69*, 154–164. [CrossRef]

Disclaimer/Publisher's Note: The statements, opinions and data contained in all publications are solely those of the individual author(s) and contributor(s) and not of MDPI and/or the editor(s). MDPI and/or the editor(s) disclaim responsibility for any injury to people or property resulting from any ideas, methods, instructions or products referred to in the content.